

# Deformation and metamorphism at the eastern border of the Tenda Massif (NE Corsica): a record of subduction and exhumation of continental crust

G. Molli <sup>a,c,\*</sup>, R. Tribuzio <sup>b,c</sup>, D. Marquer <sup>d</sup>

<sup>a</sup> *Dipartimento di Scienze della Terra, Università di Pisa, Via S.Maria 53, I-56126 Pisa, Italy*

<sup>b</sup> *Dipartimento di Scienze della Terra, Università di Pavia, Via Ferrata 1, I-27100 Pavia, Italy*

<sup>c</sup> *CNR Istituto Nazionale di Geoscienze e Georisorse, Via S.Maria 53, I-53126 Pisa, Italy*

<sup>d</sup> *EA2642 Géosciences, Université de Franche-Comté Géosciences, 16 route de Gray, F25030 Besançon Cedex, France*

Received 15 February 2006; received in revised form 1 June 2006; accepted 30 June 2006

Available online 15 September 2006

## Abstract

A major detachment fault related to the post-orogenic extensional process and linked with rifting and drifting stages of the Liguro-Provençal and Northern Thyrrenian sea, is described in recent literature for the eastern border of the Tenda Massif, North East Corsica, Western Mediterranean. New field mapping, meso/microstructural analyses and petrological investigations have been carried out in this area. Along the eastern border of the Tenda Massif, continental and oceanic units with epidote-blueschist facies metamorphic peak conditions are juxtaposed. After their coupling in a deeper part of the Alpine Corsica subduction wedge, the two units were deformed together by greenschist facies folding and shearing.

Structural geometries and metamorphic records of the studied units, the regional tectonic settings and the available thermochronological data disclaim recent interpretations and suggest only a post-orogenic extensional reactivation. The main greenschist facies fabric and structures were related to syn-orogenic processes in response to intra-wedge deformation and strain delocalization during exhumation in a continental subduction setting.

© 2006 Elsevier Ltd. All rights reserved.

*Keywords:* Tectonics; Shear zones; Corsica; Alpine; High-pressure; Metamorphic evolution; Continental crust; Subduction; Exhumation

## 1. Introduction

Exhumed regional scale fault zones commonly show evidence for a long geological history often reflected by the complex geometry of deformation and/or superimposed fabrics recording accommodation of successive crustal deformation phases (e.g. Schmid et al., 1989; Marquer et al., 1996; Holdsworth et al., 1997; Nussbaum et al., 1998 and references therein). Superimposed fault-related fabrics with contrasting

kinematic features (shear direction and shear sense), however, can be the result of a non-steady flow produced by a progressive deformation history, heterogeneously developed during changing boundary conditions (plate tectonic or orogenic-scale), changes in metamorphic conditions (e.g. structural level) and/or rock rheology through time (Passchier, 1984; Baudin et al., 1993; Jiang and White, 1995; Passchier, 1997; Jiang and Williams, 1999).

The eastern border of the Tenda Massif is described as a regional scale fault zone, the East Tenda Shear Zone of Jolivet et al. (1990), with a quite long (>20 Ma) and complex kinematic history. It was interpreted in terms of a thrust zone related to the emplacement of the ocean-derived “Schistes Lustres” on the Corsican continental crust under HP/LT

\* Corresponding author. Dipartimento di Scienze della Terra, Università di Pisa, Via S.Maria 53, I-56126 Pisa, Italy. Tel.: +39 50 221 5749.

E-mail addresses: gmolli@dst.unipi.it (G. Molli), tribuzio@crystal.unipv.it (R. Tribuzio), didier.marquer@univ-fcomte.fr (D. Marquer).

metamorphic conditions by Faure and Malavieille (1980), Mattauer et al. (1981), Gibbons and Horak (1984), Warburton (1986). More recently, Jolivet et al. (1990) proposed a two stage history with an early thrust-related deformation (the kinematics of which is considered unclear by Jolivet et al., 1998; Rossetti et al., 2002) and a younger eastward shearing event. The latter was associated with retrograde metamorphism that began under low-pressure greenschist facies conditions and terminated at subsurface structural level (Jolivet et al., 1990; Fournier et al., 1991; Daniel et al., 1996; Gueydan et al., 2003). In this view, the major thrust fault of Mattauer et al. (1981) is considered to be a strongly or completely reactivated crustal scale structure active as a detachment fault during the Late Oligocene–Early Miocene regional scale extensional process affecting the Corsican belt. Within this framework, the Tenda Massif is considered and modelled as a post-orogenic metamorphic core complex of Cordilleran Type (Gueydan et al., 2003; Rosenbaum et al., 2005). Our contribution aims to present results of new structural investigations coupled with petrological and microstructural studies, which allow us to discuss the geometry of deformation, the kinematic history and the tectonic significance of the East Tenda Shear Zone.

## 2. Geological background of North East Corsica

Alpine Corsica (Fig. 1) shows a complete structural building of oceanic and continental upper crust units metamorphosed at different structural levels, as the result of the Mesozoic–Cenozoic convergence between the Iberian, European and African plates and the resulting closure of the Ligurian Tethys ocean (Mattauer et al., 1981; Lagabrielle, 1987; Molli and Tribuzio, 2004 and references). During the Oligocene and Miocene, the northwest Mediterranean area including the Corsican belt was affected by a regional scale extensional process leading to the rifting and oceanization of the Liguro-Provençal basin (30–16 Ma) and the following formation of the Tyrrhenian sea (16 Ma–present) (Faccenna et al., 1997; Gueydan et al., 1997; Jolivet et al., 1998; Doglioni et al., 1998; Speranza et al., 2002; Rollet et al., 2002).

Four major composite units are traditionally recognized in North Corsica (Mattauer et al., 1981; Durand-Delga, 1984; Malavieille et al., 1998). From bottom to top (Fig. 1b): (1) the “autochthonous” and “parautochthonous” Corsica (external continental units), which mainly consists of Hercynian granitoids with minor relics of host-rock basement and series of sedimentary rocks of Permian to Mesozoic ages. These external units were affected by Alpine-age deformation that occurred at low temperature and low to high pressure greenschist metamorphic conditions; (2) the strongly deformed part of the Corsican continental margin, i.e. the Tenda Massif and the more internal Centuri/Serra di Pigno/Farinole units, with peak metamorphic conditions in the epidote-blueschist to eclogite facies and widespread greenschist facies re-equilibration; (3) the ‘Schistes Lustres’ composite nappe formed by Ligurian Tethys-derived ophiolitic sequences (mantle ultramafics, gabbros, pillow lavas and associated Jurassic to Cretaceous

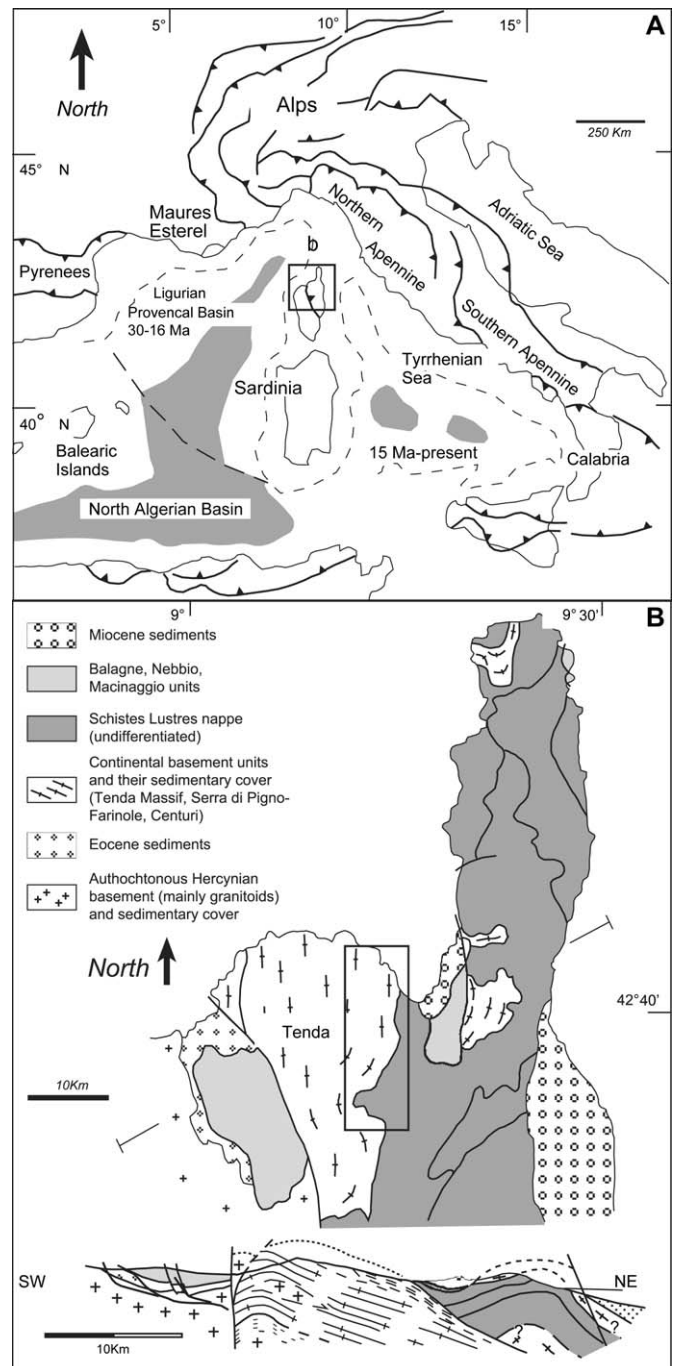


Fig. 1. (a) Tectonic setting of Corsica within the western Mediterranean; and (b) Tectonic sketch map and schematic cross section of northern Corsica showing the main tectonic units and their geometry within the nappe stack. Rectangle indicates location of the studied area.

metasediments), with peak metamorphism of epidote- to lawsonite-blueschist and eclogite facies conditions, variably retrogressed to greenschist facies; and (4) the Balagne/Nebbio/Macinaggio system represented by ophiolitic and continental units, characterized by prehnite-pumpellyite assemblages in mafic rocks (Dal Piaz and Zirpoli, 1979; Pequignot et al., 1984; Bezert and Caby, 1988; Fournier et al., 1991; Caron, 1994; Malasoma et al., 2006). The uppermost nappes and their contact with the underlying units are unconformably sealed by

Early Miocene marine sediments, e.g. the St. Florent, Francardo, Aleria basins (Dallan and Puccinelli, 1995; Ferrandini et al., 1998).

### 3. Structural geometries and metamorphism in the Tenda Massif and ophiolitic unit

#### 3.1. The Tenda Massif

The Tenda Massif forms an elongate culmination of continental-derived metamorphic rocks interposed between the western external units (“autochthonous” and “paraautochthonous”) and the Balagne nappe, and the eastern “Schistes Lustrés” composite nappe system. The massif mainly consists of a core of Late Hercynian granitoids surrounded by orthogneisses deformed during Alpine tectonics. The Late Hercynian granitoids include gabbroic intrusions of Lower Permian age (e.g. the Bocca di Tenda gabbro), and both granitoids and gabbros are locally crosscut by basalt to rhyolite dykes (Ohnenstetter and Rossi, 1985; Rossi et al., 1992). Scattered remnants of pre-Hercynian low-grade basement rocks are also present (Rossi et al., 1994). A metasedimentary cover, deposited from Permian to Mesozoic times, discordantly overlies the basement rocks (Durand-Delga, 1984; Rossi et al., 1994, 2003).

The study area is located at the eastern border of the Tenda Massif (Fig. 1b), in the eastern limb of a large-scale antiform showing an amplitude around 20 km in the North, between S.Florent and Ostriconi, and less than 5 km at the southern periclinal termination north of Ponte Leccia. The finite geometry of the elongate dome is related to the activity of a major system of wrench faults (mainly post-Eocene and pre-Burdigalian in age) described at the western boundary of the Tenda Massif, along the contact with the Balagne nappe (Central Corsica Fault zone of Maluski et al., 1973; Waters, 1990), and in the southern-east part of the massif (Waters, 1990; Rossi et al., 2003). According to Jourdan (1988), Waters (1990) and Molli and Tribuzio (2004), the domal antiform modifies a previously developed antiformal stack (see below).

Structures related to a polyphase deformation history are widely observable in cover rocks of the Tenda Massif, where at least two generations of isoclinal folds are overprinted by a late phase developing open and kink folds. On the contrary, basement rocks commonly exhibit a simpler structural history. In particular, a regional-scale main foliation wrapping up preserved undeformed domains (meter to kilometer in scale e.g. Casta granodiorite of Rossi et al., 1994) can be recognized in granitoids. The main foliation is generally characterized by greenschist facies assemblages, although relict domains of pre-greenschist structures can be found (see below). On the basis of shear directions, overprinting relationships and petrologic data, the structures formed under greenschist facies metamorphic conditions have been subdivided into two groups, interpreted as developed at different depth (Molli and Tribuzio, 2004). The younger structures D3 (“GS2” by Molli and Tribuzio, 2004) are characterized

by localized zones of deformation from centimeter to meter in size, forming shear band systems associated with north-east/southwest trending stretching and mineral lineations (Fig. 2a) and top-to-the northeast shear sense indicators (Fig. 3a,b). These structures can be easily recognised toward the eastern border of the Tenda Massif, where they were firstly described by Waters, 1990 and Jolivet et al. (1990); see also Daniel et al., 1996; Egger and Pinaud, 1998; Gueydan et al., 2003. D3 structures are also present inside the massif, where conjugate shear zones were described by Molli and Tribuzio (2004) and interpreted as related to partitioned coaxial strain and vertical shortening far from the eastern border of the Tenda Massif.

D3 fabrics in granitoids are associated with celadonite-poor phengite (Si = 3.2–3.3 apfu, Fig. 4a) + epidote + albite + quartz ( $\pm$ chlorite  $\pm$  calcite) assemblages. The dolerite dykes developed chlorite + albite + epidote ( $\pm$ phengite  $\pm$  quartz  $\pm$  calcite). Metabasites are thus characterized by the absence of amphibole and can be related to the “lowermost greenschist facies” (Spear, 1993). As a whole, these mineral assemblages indicate that the D3 deformation occurred at temperatures of 300–400 °C and pressures lower than 0.5 GPa.

Meter- to pluridecameter-sized D3 open to close folds associated with sub-horizontal to medium steep crenulation cleavage can be locally observed. They commonly show fold axes sub-parallel to the stretching lineation of the surrounding D3 shear zones (Fig. 3c). Semi-brittle shear bands and cataclasis-bearing fault zones (late- and post-D3 structures) geometrically and kinematically coherent with D3

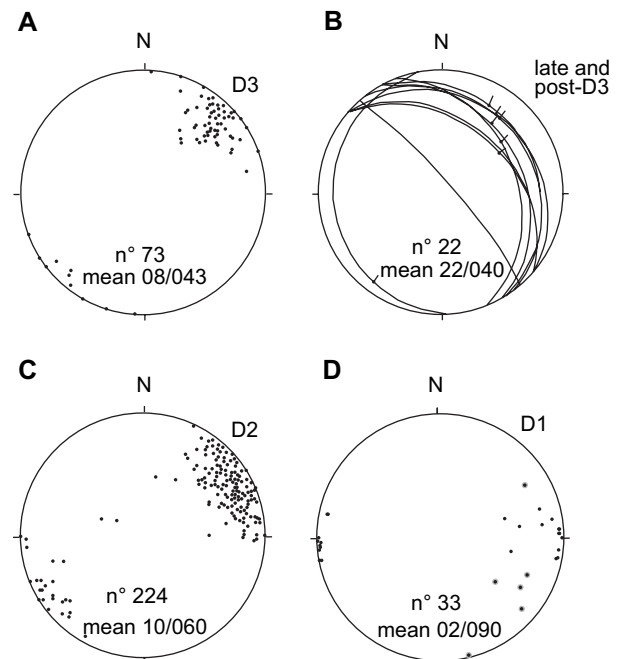


Fig. 2. Equal area projection plots (lower hemisphere) of: (a) stretching/mineral lineation of D3; (b) late- and post-D3, great circles for shear bands and slicklines; (c) D2 and (d) D1 stretching/mineral lineations. In (d) black dots and mean trend refer to lineation in D1 domains unaffected by D2/D3 overprint, whereas black dots with grey rims refer to D1 lineation in relict domains within D2 or D3 dominant fabrics.

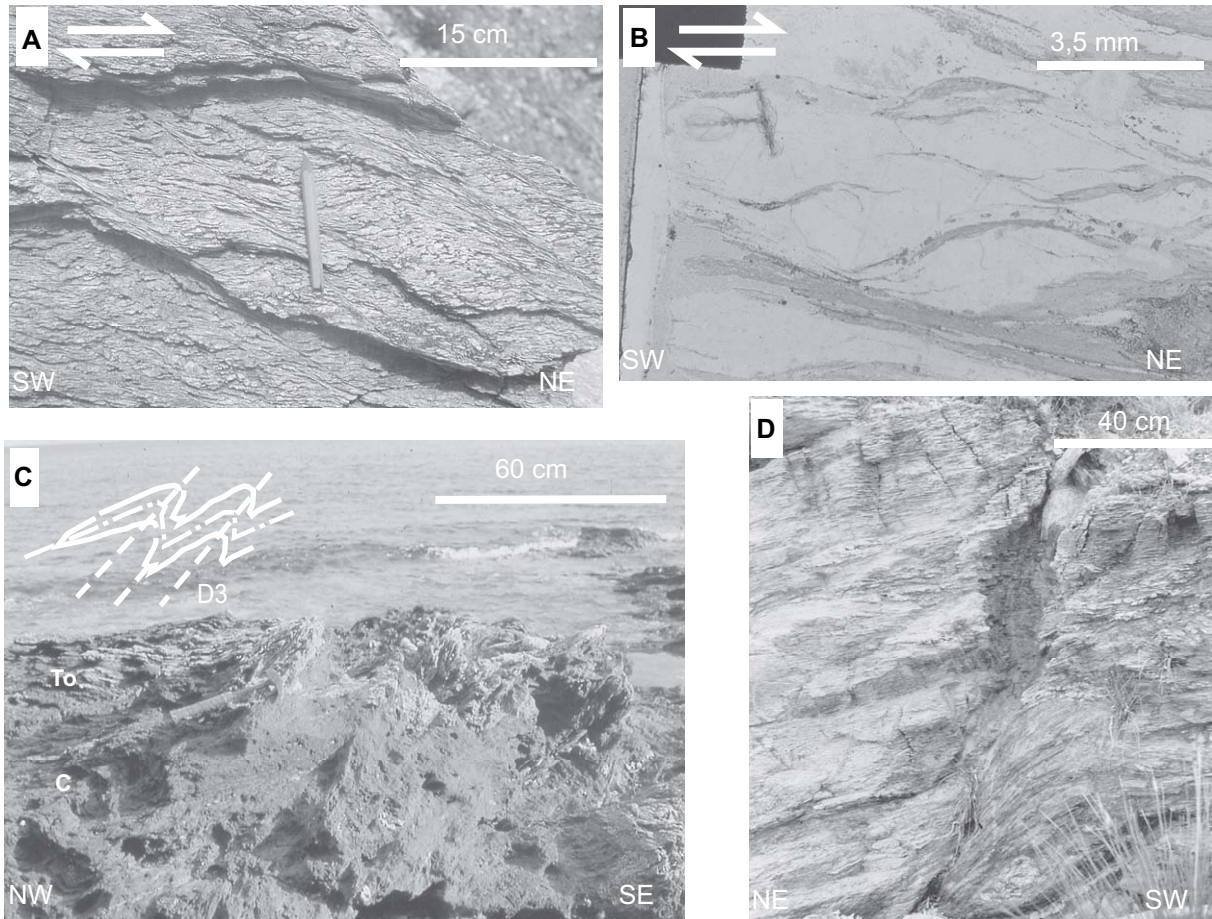


Fig. 3. (a) D3 shear bands in granitic mylonites observed on XZ plane of finite strain ellipsoid; (b) photomicrograph of XZ thin section under natural polarized light, sample 86; (c) asymmetric southeast vergent D3 folds refolding D2 isoclinal folds at the contact between Tenda orthogneiss (To) and ophiolitic calcschists (c) East Calaverite bay; and (d) post-D3 brittle fault, coast-line west of S.Florent.

structures are locally present (Figs. 2b and 3d). They are interpreted as related to a progressive deformation at lower temperature conditions in the uppermost crust. D3 structures therefore evolved toward shallower depths with late- and post-D3 structures.

The main fabric along the eastern border of the Tenda Massif (as well as inside it) can be attributed to the D2 stage of greenschist facies deformation (“GS1” by Molli and Tribuzio, 2004). This fabric shows stretching and mineral lineations (Fig. 2c) oriented east-northeast/west-southwest (mean attitude toward 60°). Shear sense indicators such as asymmetric porphyroclasts and shear band systems of C- and C'-type show both top-to-west (southwest) and predominant top-to-east (northeast) kinematics (Fig. 5a–d). D2 structures in granitoids are associated with celadonite-rich phengite (Si ~ 3.5 apfu, Fig. 4a) + epidote + albite + quartz (± calcite ± chlorite ± actinolite) assemblages. Quartz microstructures (Fig. 5c) show typical features of recrystallisation regime 3 of Hirth and Tullis (1992); recrystallised grains (mean grain size around 0.05–0.1 μm) formed by both grain boundary migration and sub-grain rotation.

Mafic dykes within orthogneiss show locally (e.g. at Bocca di Spizzico, kilometric coordinate 567.4/264.2; near the

contact with the Casta Granodiorite, kilometric coordinate 655.6/263.6 and in the Pilocaccia area kilometric coordinate 568.2/263.3) a D2 fabric characterized by spaced crenulation with large Na-amphibole in the microlithons (D1 relicts see below) and fine-grained Na-amphibole in the crenulation. This finding has thus indicated that D2 deformation started under blueschist facies conditions. The rather high celadonite content of phengites from D2 orthogneisses is consistent (e.g. Massonne and Schreyer, 1987) with a deformation event that started at relatively great depth. Remarkably, the fine-grained Na-amphibole in the crenulation of the mafic dykes shows an outward decrease of Al contents, thus suggesting that the D2 blueschist facies evolution, which preceded the transition to the greenschist facies stability field, was associated with a pressure decrease (cfr. Egger and Pinaud, 1998).

Mafic rocks recording D2 deformation under greenschist facies conditions are also present and characterized by a paragenesis of actinolite + albite + chlorite + epidote + phengite. In particular, we have found a microgabbro body (Rue de Morello bridge along the D62, kilometric coordinate 567.7; 263.2) displaying two generations of greenschist facies amphibole (Fig. 6). The earlier one (Act 1) occurs as coronas around

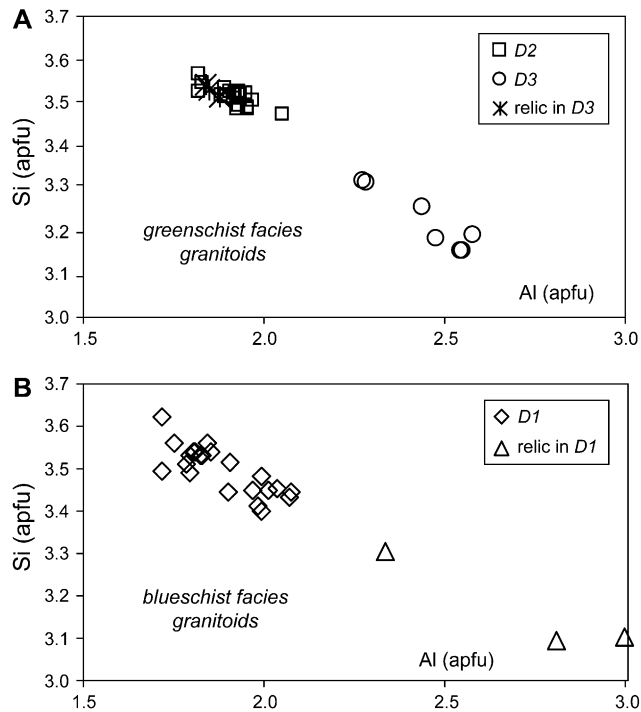


Fig. 4. Phengite compositions from metagranitoids deformed under greenschist (a); and blueschist (b) facies conditions; Si vs.  $Al_{tot}$  (atoms per formula unit, apfu). D1, D2 and D3 = phengites related to D1, D2 and D3 fabrics, respectively.

Ti-pargasite of igneous origin. Such coronitic structures are involved in top-to-west shear band systems characterized by recrystallisation of actinolite (Fig. 5d). The amphiboles developed in the shear bands (Act 2) have lower Na/Ca + Na, Al/Al + Si and Ti than Act 1 (Fig. 6a,b). These compositional variations indicate (e.g. Spear, 1993) that the greenschist facies evolution predating the D3 event was characterized by a concomitant decrease of both pressure and temperature conditions. As a whole, the different parageneses and mineral compositions developed in mafic rocks recording the D2 deformation provide evidence for a decompression evolution associated with a temperature decrease.

Widespread relics of pre-greenschist facies assemblages and structures (D1) can be observed all along the eastern border of the Tenda Massif (Fig. 7). For instance, a well accessible exposure is located near Fontana Porrighia (Figs. 7–9), along the D62 (kilometric coordinate 567.5/262.07). In this outcrop, the orthogneisses show a main foliation defined by Na-amphibole (Fig. 9a,b) + celadonite-rich phengite (Si ~ 3.5 apfu, Fig. 4b) + epidote + albite + quartz ( $\pm$ chlorite  $\pm$  K-feldspar). White mica cores locally preserve celadonite- (Si = 3.1–3.3 apfu) and Ti-poor compositions (Fig. 4b), which can be attributed to a low-pressure stage of the prograde path. Mineral relics that can be referred to the prograde metamorphic evolution were also found in the blueschist facies mafic rocks from the Bocca di Tenda area (kilometric coordinate 565/252) (Tribuzio and Giacomini, 2002). In this area, orthogneisses and mafic rocks with epidote-blueschist facies mineral assemblages are common (Lahondère et al., 1999) and

associated with blueschist facies meta-rhyolites displaying jadeite-bearing aegirine, Na-amphibole, celadonite-rich phengite, quartz, albite and K-feldspar (Tribuzio and Giacomini, 2002), and Mg-rich gabbros with epidote-amphibolite facies metamorphic peak assemblages (Al-poor hornblende, celadonite-rich phengite, epidote and albite; Molli and Tribuzio, 2004). The different high-pressure parageneses from the Bocca di Tenda rocks permitted to estimate the peak metamorphic conditions at  $450 \pm 50$  °C and  $1.0 \pm 0.1$  GPa (Tribuzio and Giacomini, 2002; Molli and Tribuzio, 2004). This agrees with the previous estimates of Egger and Pinaud (1998), who gave peak temperature and pressure conditions of 350–450 °C and 0.8–1.4 GPa.

The blueschist-facies fabric shows lineations of mineral (Na-amphibole) and stretching (quartz aggregates) types oriented east-west (mean toward  $268^\circ$ ), with top-to-west kinematics well defined by asymmetrical porphyroclast systems of  $\sigma$ -type and widespread shear band systems in metadolerites (Figs. 9a–c). Centimeter to decimeter-scale E-vergent folds deforming the blueschist foliation can be observed in orthogneisses interposed between mylonitic metadolerites (Fig. 8e). The Na-amphibole fabric around the folds is not retrogressed to greenschist-facies assemblages, thus allowing us to interpret the folds as related to the back-rotation of blueschist foliation in a progressive history of top-west shearing. This event possibly occurred during the development of shear bands in metadolerites, in the latest stages of blueschist shearing. Fig. 8g illustrates fold/shear zone relationships as observed from decimeter to microscale and their interpretation according to the model described by Harris et al. (2002).

The blueschist foliation grades to orthogneisses characterized by greenschist facies assemblages, and the transition shows a gradual variation normal to the foliation and along the strike. Toward the west, the blueschist facies foliation coplanarly grades to a greenschist foliation characterized by a well-developed lineation of stretching and mineral type oriented toward southwest ( $248^\circ$ ) (Fig. 8b). In this domain, asymmetric porphyroclast systems and well-developed shear bands define a top-southwest kinematics (Fig. 8d). East of Fontana Porrighia, the transition to greenschist foliation occurred through a decameter thick domain of strongly crenulated orthogneisses. This domain shows the partial to total breakdown of blueschist facies Na-amphibole (Fig. 8f).

### 3.2. The ophiolitic unit

At its eastern border the Tenda Massif is in contact with a typical ophiolitic unit formed by serpentinites, metabasites and a metasedimentary cover (Figs. 1b, 7 and 10). The latter shows significant variations from northernmost to southernmost exposure areas. In the North, the metabasites are stratigraphically followed by quartzitic-micaschists and calcschists, whereas pure quartzites, marbles and calcschists crop out to the South near S. Pietro di Tenda, at the south-eastern edge of the Tenda Massif. Our observations and cross-sections (Fig. 11) support the proposal of Caron and Delcey (1979),

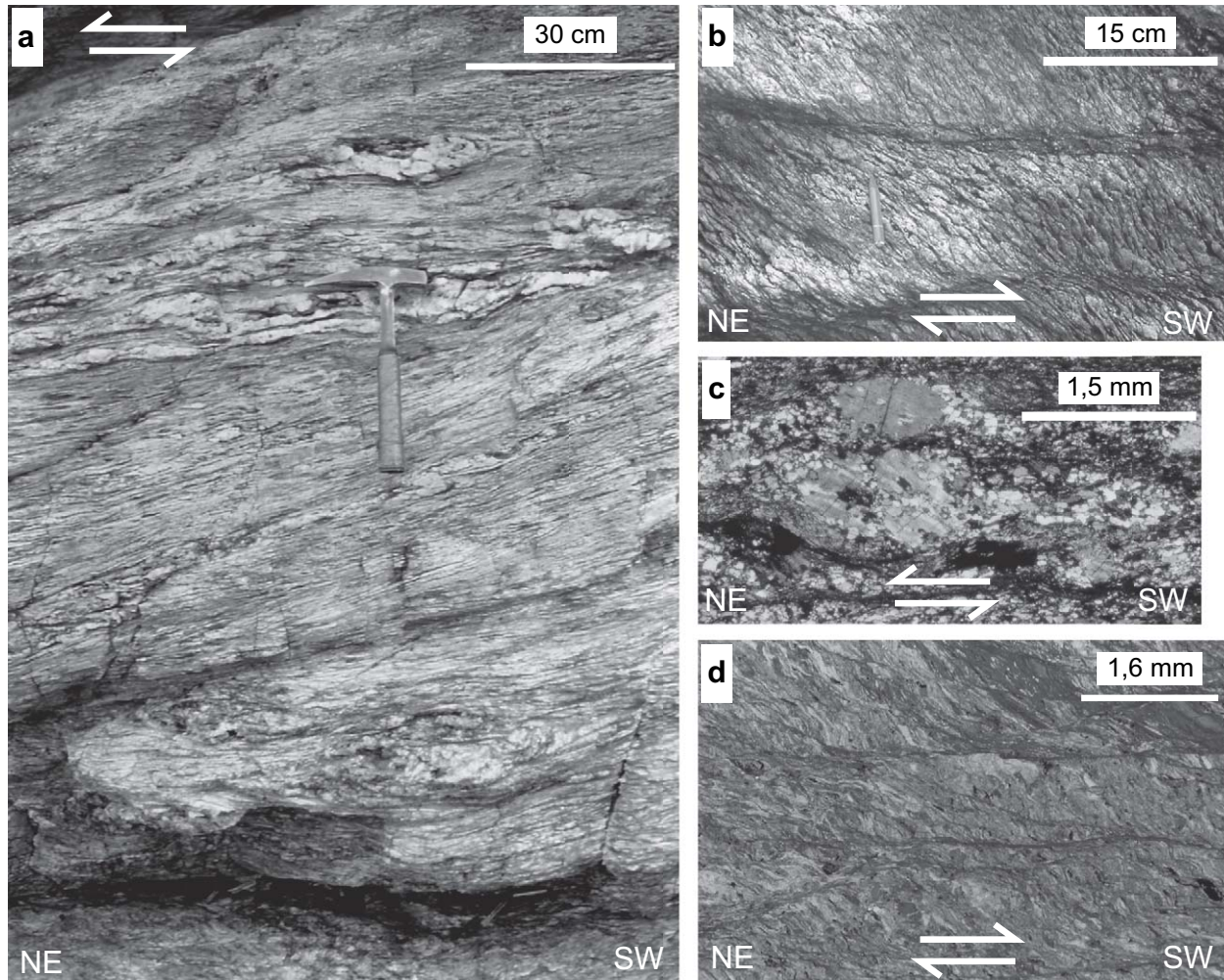


Fig. 5. (a) D2 structures with well developed top-to-northeast shear sense indicators (asymmetric porphyroclasts, asymmetric mylonitic folds and shear bands); (b) decimeter-scale S/C structures pointing to a top-to-southwest shearing in granitic mylonite; (c) cross polarized micrograph of granitic mylonite with dynamically recrystallized quartz, sample Te 70; (d) mylonitized portion of microgabbro dyke (sample Te102) showing top-to-southwest shear bands observed along the D62 at Rue de Morello bridge (567.7; 263.2).

who considered the Santo Pietro di Tenda sequence as a Late Jurassic-Cretaceous ophiolite-cover. The presence of continental-derived debris in carbonates, which led Warburton (1986) and Durand-Delga (1984) to consider the Santo Pietro di Tenda sequence as a Mesozoic continental crust cover unit is, in our view, the result of the influx from a nearby continental margin, similar to what is documented in other Corsica ophiolitic units (e.g. Durand-Delga, 1984; Lahondère, 1991; Marroni and Pandolfi, 2003 and references therein).

The peak metamorphic assemblages in the metabasites derived from lava flows are characterized by Na-amphibole + albite + chlorite + epidote + phengite ( $\pm$ calcite). The metabasalts therefore display typical epidote-blueschist facies (Evans, 1990) assemblages, similar to those observed for the metadolerites within the Tenda orthogneisses and for the metadiorites from the Bocca di Tenda gabbroic sequence (Tribuzio and Giacomini, 2002; Molli and Tribuzio, 2004). In the ophiolite unit, blueschist facies metabasites derived from Fe-Ti-rich gabbroic protoliths have also been found, for instance at Monte S. Angelo (kilometric coordinate 566.9/249). These

rocks commonly preserve mineral relics of the igneous paragenesis (i.e. ilmenite and Ca-clinopyroxene, (Fig. 12) and display a peak metamorphic assemblage of Na-amphibole + aegirine + albite + chlorite. Ophiolitic Mg-Al-rich gabbros have also been recognised and are characterized by the absence of Na-amphibole, similar to the olivine gabbro-norites from the Bocca di Tenda gabbroic sequence (Tribuzio and Giacomini, 2002). Remarkably, Na-amphiboles from blueschist facies metabasites of the Tenda Massif and the ophiolitic unit are chemically similar (Fig. 12). As a whole, these paragenetic resemblances indicate that the Tenda Massif and the ophiolitic unit underwent similar peak metamorphic conditions.

The blueschist facies assemblages in metabasites are commonly partially overprinted by greenschist facies parageneses, with development of chlorite + albite + epidote ( $\pm$ phengite  $\pm$  calcite  $\pm$  actinolite). A widespread re-equilibration under greenschist facies conditions is commonly shown by the ophiolitic metasediments. Nevertheless, peak metamorphic assemblages that can be referred to the blueschist facies are locally preserved; for instance, quartzitic-micaschists from Calaverte bay

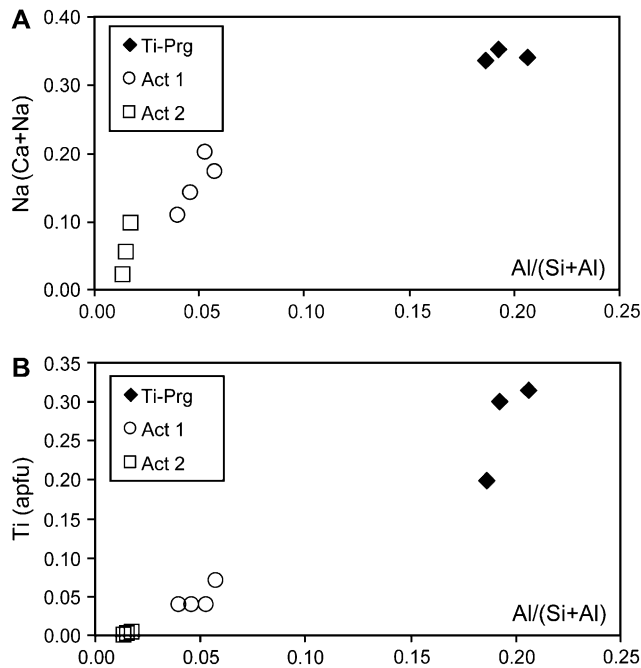


Fig. 6. Amphibole compositions from Tenda microgabbro with greenschist facies metamorphism, involved in the D2 deformation event. Na/(Ca + Na) vs. Al/(Si + Al) and Ti vs. Al/(Si + Al) in apfu. Ti-Prg = Ti-pargasite of igneous origin; Act 1 = actinolite in coronas around Ti-Prg; Act 2 = actinolite in top-to-west shear band systems (D2 event).

display a relict paragenesis of Na-amphibole + quartz + phengite + albite. The ophiolitic unit is characterized by distributed deformation associated with pervasive folding from cartographic to thin section scale (Figs. 9d,f and 11). Two generations of isoclinal folds (D1 and D2) are associated with the two major stages of metamorphism (under blueschist and greenschist facies conditions, respectively), whereas later stages of folding are characterized by sub-horizontal to sub-vertical axial-planar disjunctive crenulation cleavage and kink bands (D3 and late-D3; Figs. 3c and 9d). Map and cross-sections of Figs. 7 and 11 highlight the superimposed structures observable in the ophiolitic unit around Santo Pietro di Tenda.

### 3.3. The geometries of the contact between the Tenda and the ophiolitic unit

The geological maps of Figs. 10 and 13 describe in some details the geometries of the contact between the Tenda and the ophiolite unit west of S.Florent village. Key exposures are to be found South of the Fornali lighthouse (cf. Waters, 1990; Dallan and Puccinelli, 1995), where it is possible to observe an orthogneiss and mylonitized volcano-sedimentary cover (Tenda-derived) overlying the ophiolitic unit here formed by metabasites and calcschists. Between Fornali and Punta Cepu, the orthogneiss and the mylonitized Tenda-derived cover show pervasive isoclinal folds at different scales and strongly curved intersection lineations on foliation planes (Fig. 14a). The axial planar foliation of the isoclinal

folds shows greenschist facies assemblages with phengite composition (Si = 3.4–3.5 apfu) similar to D2 structures in other parts of the Tenda.

Further North, in the Calaverte bay (Figs. 10 and 13a–c), the ophiolitic unit reappears with a sequence of tremolite schists (possibly mantle-derived ultramafics), metabasites, quartzitic-micaschists and calcschists forming tight folds within the orthogneiss (Fig. 14c). Meso- and microstructural features show that the axial planar foliation of the folds is associated with greenschist assemblages deforming an older blueschist fabric. These two foliations (and the associated isoclinal folds D1 and D2) are both deformed (Figs. 9d and 14d) by west-dipping disjunctive crenulation cleavage axial planar of metric scale east-vergent open to close folds (D3). We interpret the exposure of the Calaverte Bay as associated with the lateral termination of a strongly non-cylindric recumbent fold (Figs. 13b and 15). The ophiolitic unit (calcschists and metabasites) is pinched within the orthogneisses, which therefore were more competent during deformation. These structures are considered as being due to the buckling of the original thrust contact (with the ophiolitic unit arranged in an inverted limb of a kilometer-scale west vergent isoclinal D1 fold above the Tenda orthogneiss, Fig. 11b), followed by rotation and strain of the earlier fold during south-west/northeast directed shearing. Similar geometries of deformation can be also observed South of S.Pietro di Tenda, around the M.Buggentone area (kilometric coordinate 567.1/252.1) and further south, in the Ponte Leccia surroundings (kilometric coordinate 568/244). Therefore, at the scale of the whole eastern border of the Tenda, the contact between the continental Tenda and the ophiolitic units appears tightly folded in large scale recumbent D2 sheath folds (Figs. 11b, 13b and 15).

### 3.4. Deformation and metamorphic evolution of the units across the Eastern border of the Tenda Massif

Fig. 16 reports the P-T-t-d evolution of the units in contact across the eastern border of the Tenda Massif. Both oceanic and continental (Tenda) units are characterized by peak metamorphic conditions around 450 °C and 1.0 GPa, which can be referred to the ambient conditions for D1 deformation. The mineral zoning observable in the core of white micas and Na-amphiboles records the lower pressure stages of the prograde path developed during the involvement in the subduction. D2 deformation and structures can be related to the exhumation history, which started under HP/LT metamorphic conditions and evolved toward a lower pressure environments, thus allowing the early greenschist facies assemblages to develop. The following D3 structures formed at temperature around 350 °C and pressure lower than 0.5 GPa and were overprinted at shallow structural levels by the late- and post-D3 semibrittle and brittle structures. D3 and late- to post-D3 structures are localized and correlated with low displacements (from millimeters to meters) across the single structure. In addition, their total effect is negligible at a crustal scale, as observable by the

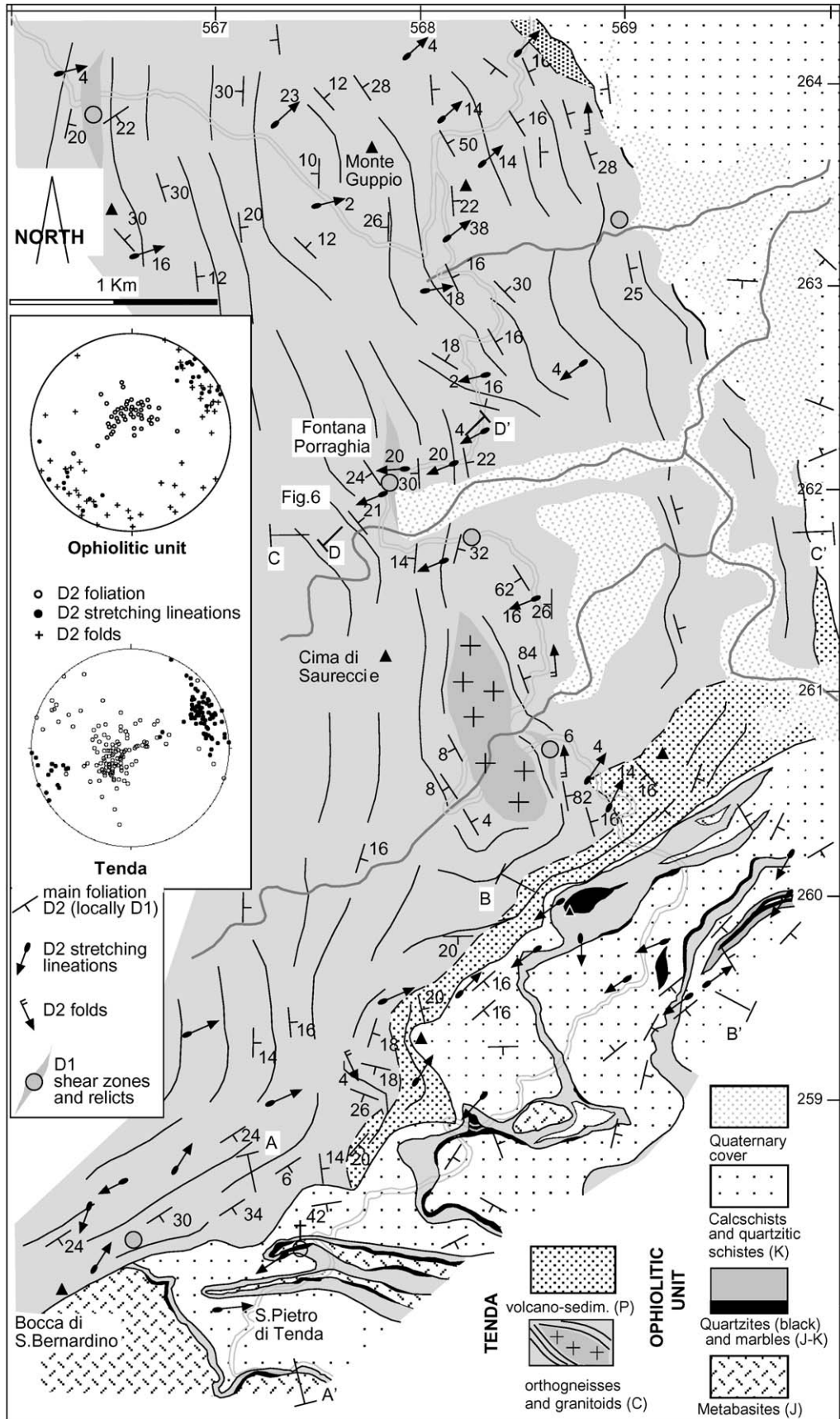


Fig. 7. Geologic sketch map of the area North of S. Pietro di Tenda, with inset of equal area projection plots (lower hemisphere) of pole of foliation, stretching/mineral lineation, and fold axes of D2 structures in the Tenda and ophiolitic units.



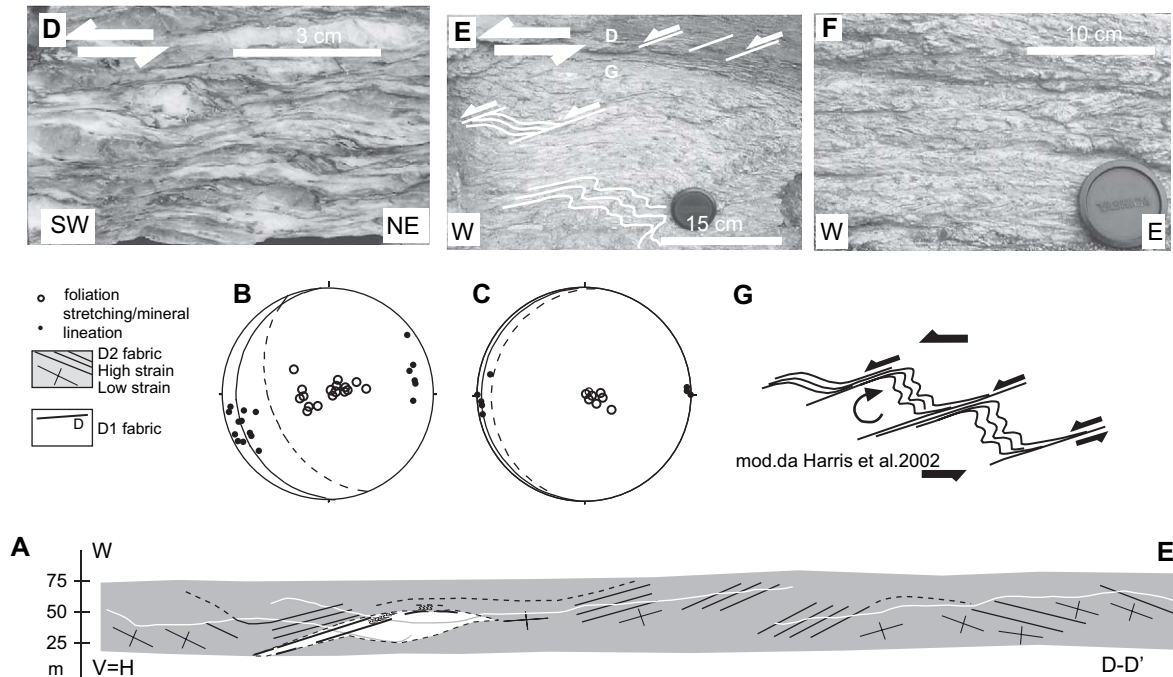


Fig. 8. (a) Cross-section of Fontana di Porraghgia and surroundings showing D1 shear zone relicts and D2 foliation with gradient of D2 strain; equal area projection plots (lower hemisphere) of pole of foliations, great circles of shear bands and stretching lineations for D1 (b) and D2 (c) deformation; (d) D2 fabric with well developed top-to-southwest shear bands; (e) contact between mylonitized dolerites (D) with top-to-west shear bands and granitic mylonites (G) with top-to-west shear bands and centimeter-scale backfolds; (f) D2 crenulation with greenschist retrogression of former D1 fabric in the microlithons; (g) schematic diagram showing development of east-vergent folds between shear band systems associated with top-to-west shearing, on the basis of Harris et al. (2002).

undisrupted geometries of D2 large scale folds affecting the contact between oceanic and continental units (Figs. 11b, 13c and 15).

#### 4. The Eastern border of the Tenda Massif: post-orogenic detachment fault or syn-orogenic shear zone?

In the last decades, criteria to recognize the crustal nature of faults and shear zones in orogens have been highlighted (e.g. Burg et al., 1984; Mancktelow, 1985; Selverstone, 1985; Platt, 1986; Malavieille, 1987; Lister and Davis, 1989; Schmid and Haas, 1989). However, in many cases the tectonic significance of the described structures remains debatable (Wheeler and Butler, 1994; Ring et al., 1999), since thermal structure, original geometry and timing of deformation are in most cases not sufficiently constrained. Yet, two first order tectonic features are characteristic of Cordilleran-type detachment faults (e.g. Crittenden et al., 1980; Wernicke, 1981; Malavieille, 1987): (i) the presence of a brittle fault surface; and (ii) a discontinuity in metamorphic conditions, between higher-grade rocks in the footwall and lower-grade rocks in the hanging wall.

The contact between the Tenda and the ophiolitic unit is considered as a sharp eastward shallow dipping fault by Jolivet et al (1990), Daniel et al. (1996) and Gueydan et al. (2003). On the basis of this interpretation, and the widespread top to east/north-east kinematics, the structure was considered as a detachment fault of Cordilleran-type

and framed within a tectonic setting of regional-scale extensional process. However, the data presented here do not fit with the described structural geometries. In addition, in contrast to what has been claimed in recent literature (for instance Jolivet et al., 1998; Rossetti et al., 2002), all along the eastern border of the Tenda Massif significant structural and petrological relics of a deep seated tectonic process associated with subduction can be found. These data solicit a reconsideration of the regional significance of the East Tenda Shear Zone proposed by Jolivet et al. (1990).

In our discussion, we shall take into account the structures along the eastern border of the Tenda Massif, as well as the overall available regional data set. A first point to focus is the age of the metamorphic events in the Tenda Massif, which is a controversial topic (e.g. Handy and Oberhänsli, 2004). A crude, two-step discordant  $^{40}\text{Ar}/^{39}\text{Ar}$  on glaucophane of about 90 Ma was interpreted by Maluski, 1977 as the age of the thermal peak. Similarly, a Rb-Sr whole-rock age of  $105 \pm 8$  Ma was considered by Cohen et al. (1981) as the age of the HP/LT metamorphic event. More recently, a separate of celadonite-rich phengites ( $\text{Si} = 3.5$  apfu) from a deformed granitoid of the Northern Tenda Massif has yielded a discordant  $^{39}\text{Ar}/^{40}\text{Ar}$  spectrum that regularly increases during step-heating, from about 25 Ma to 47 Ma (Brunet et al., 2000). According to Molli and Tribuzio (2004), this suggests that the high-pressure metamorphism had a minimum age of 47 Ma.

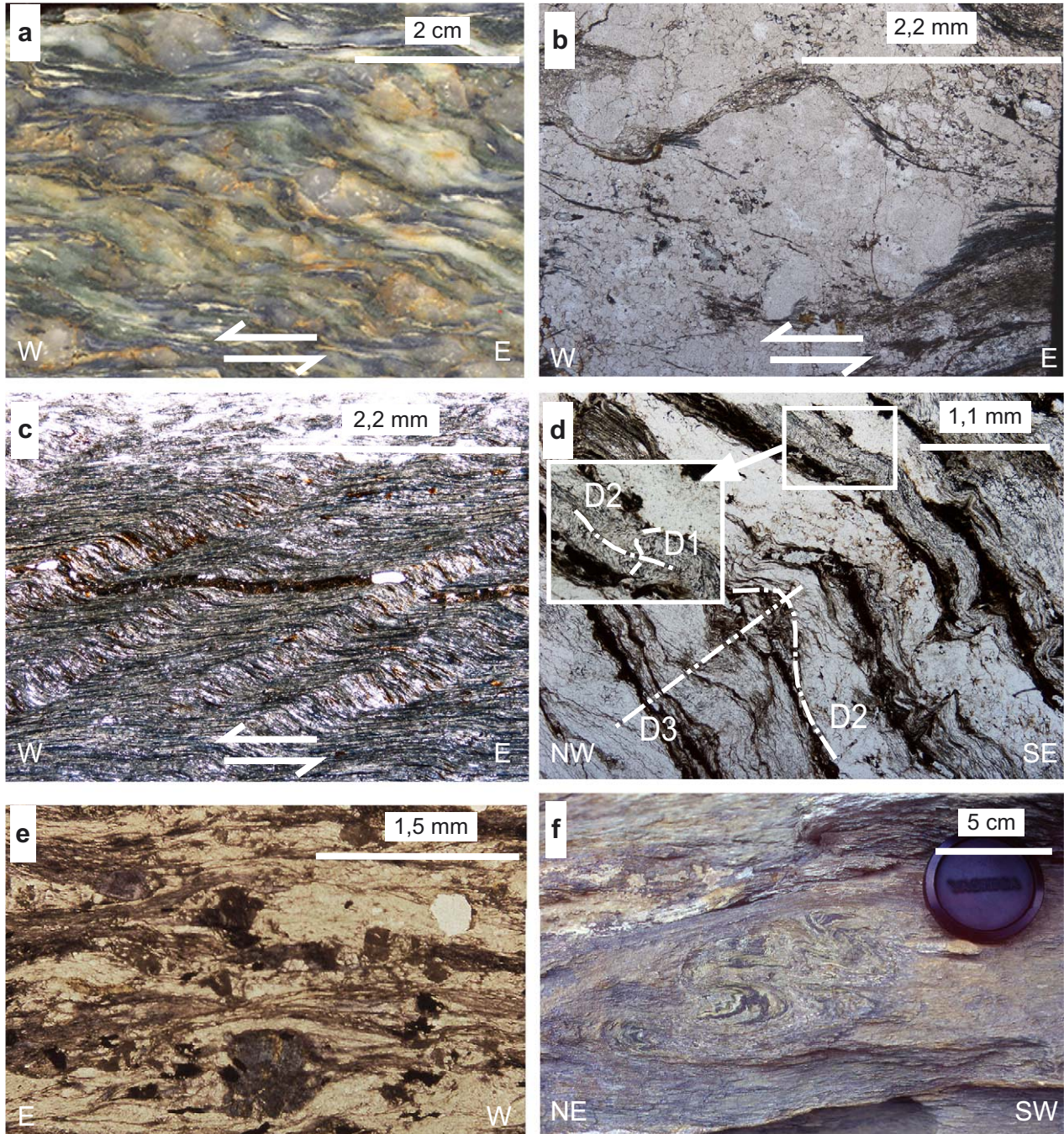


Fig. 9. (a) Blueschist facies mylonitic metagranite showing asymmetric porphyroclasts and shear bands define a top-to-west shear sense, XZ plane; (b) photomicrograph detail in natural polarized light showing syn-kinematic Na-amphibole in the tails of K-Feldspar asymmetric porphyroclast XZ plane; (c) photomicrograph of mylonitic metadolerite with a well defined shear band system pointing a top-to-west shear sense natural polarized light, sample Te71, Fontana Porraghia, XZ plane; (d) superimposed foliations in quartzitic micaschist, ophiolite cover, Calaverte bay. D1 Na-amphibole can be observed in microlithons of D2 crenulation, deformed by D3 northwest dipping spaced cleavage; (e) blueschist fabric in ophiolitic mylonitized metagabbro, XZ plane; and (f) superimposed D1/D2 fabrics on metabasites, D1 isoclinal folds are refolded by tight to isoclinal D2 folds associated with sub-horizontal greenschist facies foliation.

A Late Cretaceous to Paleocene/Early Eocene age for the subduction in the Corsican orogenic system is also supported by regional data, such as: (1) the presence of detritic glauconite in Maastrichtian sediments of North West Sardinia (Dieni and Massari, 1982; Malavieille et al., 1998); and (2) the observation that in southwestern Corsica Eocene sediments

lacking HP/LT assemblages rest unconformably on the basement of western Corsica and Schistes Lustres (Caron, 1994; Egal, 1992).

The underthrusting of the Corsican continental crust is documented to persist during the Eocene, since the external continental units of “parautochthonous” and internal part of

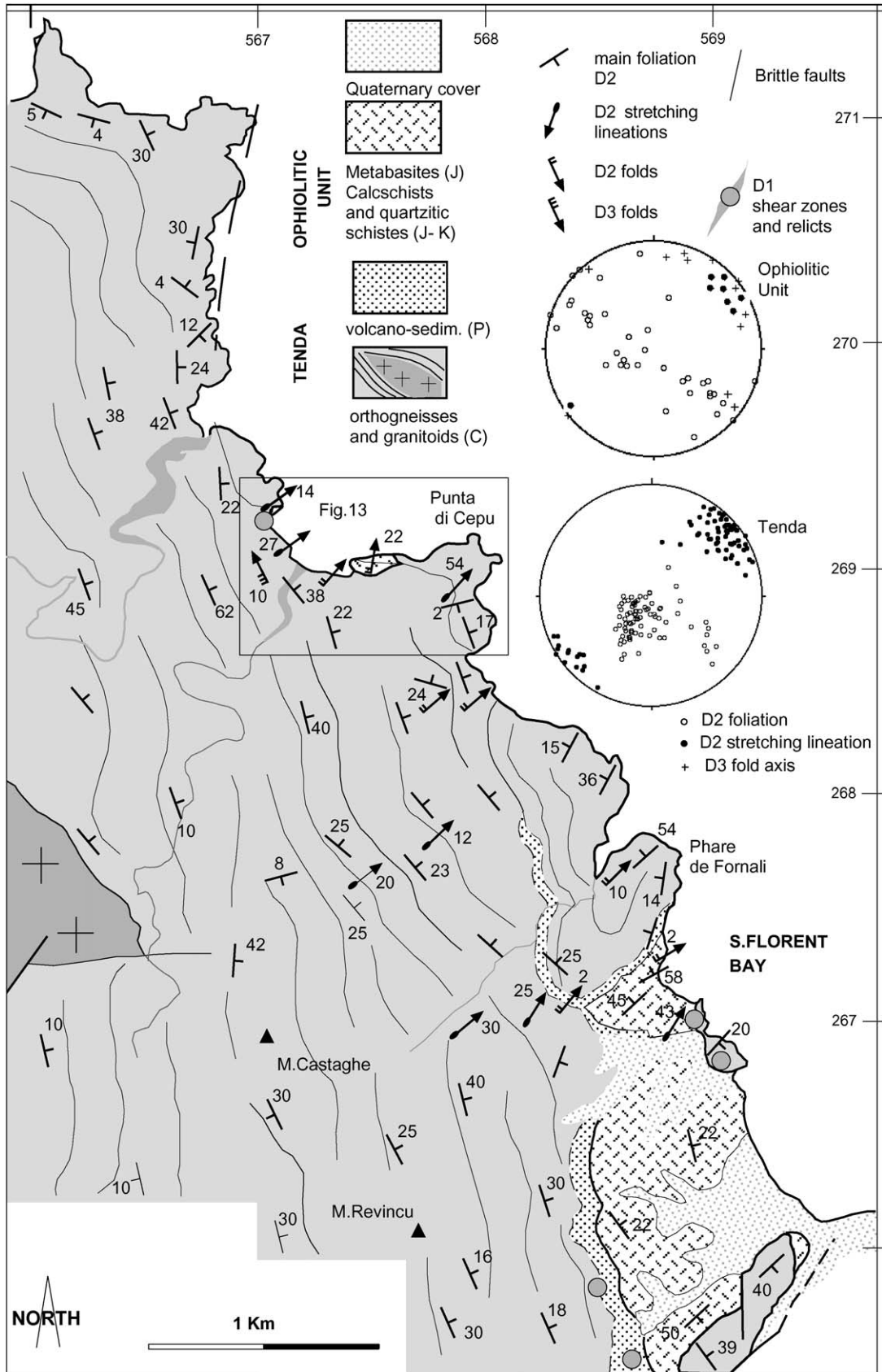


Fig. 10. Geologic sketch map of the area west of S. Florent, with inset of equal area projection plots (lower hemisphere) of pole of foliation, stretching/mineral lineation, and fold axes of D2 structures in the Tenda and ophiolitic units. Rectangle indicates the location of Fig. 13.

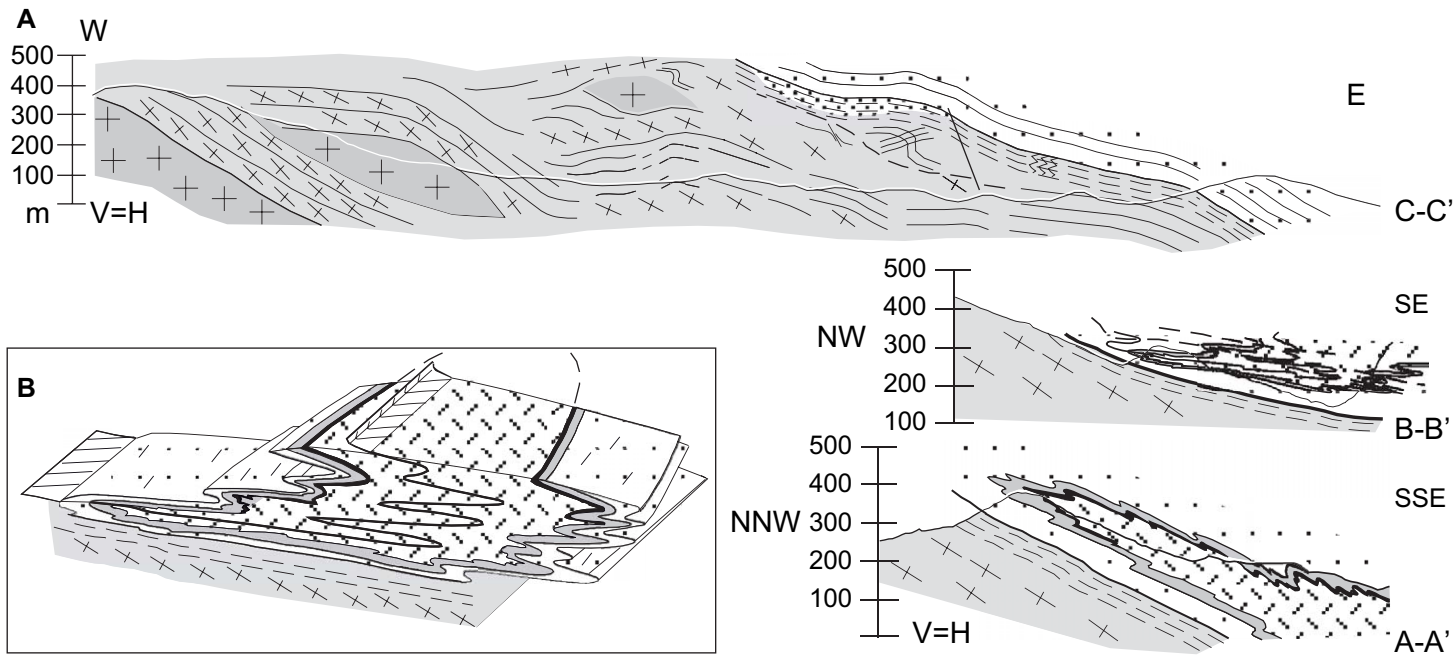


Fig. 11. Geological cross-sections at the eastern border of Tenda (traces in Fig. 7). The patterns are the same as in Figs. 7 and 10. Inset b shows schematic interpretative block diagram of structural geometries around Santo Pietro di Tenda, showing large scale D1 isoclinal fold in ophiolitic unit refolded with the Tenda unit during D2 deformation, axial trace of D1 fold in black is outlined. For A-A' and B-B' cross-sections scale is 1.2 time that of C-C'.

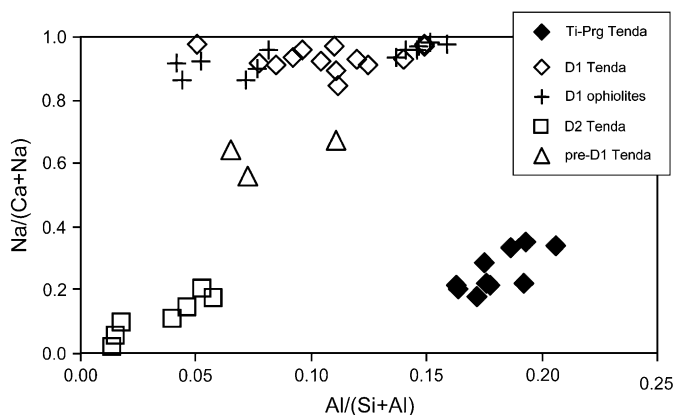


Fig. 12. Amphibole compositions from Fe-rich mafic rocks of the Tenda Massif (dolerite dykes and Qtz-diorites from the Bocca di Tenda gabbroic sequence) and associated ophiolites (deformed basalt flows and Fe-Ti-rich gabbros); Na/(Ca + Na) vs. Al/(Si + Al) in apfu. Ti-Prg Tenda = Ti-pargasites of igneous origin in Fe-rich mafic rocks from the Tenda Massif; D1 Tenda = Na-amphiboles related to D1 deformation event in Fe-rich mafic rocks from the Tenda Massif; D1 ophiolites = Na-amphiboles related to D1 deformation event in Fe-rich mafic rocks from the ophiolitic unit; D2 Tenda = amphiboles related to D2 deformation event in Fe-rich mafic rocks from the Tenda Massif; pre-D1 Tenda = prograde Na-Ca-amphiboles (winchites) in Fe-rich mafic rocks from the Tenda Massif.

the “autochthonous” are affected by HP/LT metamorphism (Bezert and Caby, 1988; Bezert, 1990; Molli et al., 2005; Malasoma et al., 2006). These units contain a sedimentary cover paleontologically dated to the early Mid-Eocene (dated on the basis of the presence of *Nummulites biarrizensis*; *Discocyclina* sp. by Bezert and Caby, 1988). Therefore, stratigraphic data from the frontal part of the Corsican wedge suggest that blueschist facies and associated underthrusting and subduction of continental crust continued until at least the Bartonian (40–37 Ma).

Ar/Ar investigations reported by Brunet et al. (2000), who analysed deformed granitoids of the eastern Tenda, show phengitic micas with intermediate Si compositions (comparable to our D2 phengites), which have given values of 39–32 Ma, whereas the low pressure phengites (compositions comparable to our D3 phengites) yielded ages in the range of 28–21 Ma (plateau age of 25 Ma). Taking into account all these data, the following tectonic scenario can be envisaged for the East border of the Tenda Massif (Fig. 17):

- Early stages of deformation (D1) developed under epidote-blueschist facies metamorphic conditions. D1 structures are recorded by localized shear zones showing top-to-west kinematics in the Tenda Massif and pervasive small to large scale isoclinal folding within the ophiolite unit. A major large-scale structure in the ophiolite unit appears to be present near the Tenda Massif, where a west-vergent recumbent fold with kilometer scale inverted limb can be reconstructed by retrodeformation of D2 structures. This subduction-related event affects the Tenda continental crust at a minimum age of 47 Ma;

- The ophiolite and the Tenda units are later deformed together during blueschist to greenschist decompression within a kilometer-scale D2 shear zone. The eastern border of the Tenda Massif represents the lower boundary of this shear zone. The upper boundary is within the overlying ophiolite nappes stack. The D2 event is synchronous with the underthrusting of the more external continental units (“paraautochthonous” and internal part of “autochthonous”), whose deformation can be constrained as occurred post Mid-Eocene (40–33 Ma) by the stratigraphic age of youngest sediments. Radiometric ages between 39 and 32 Ma in the eastern border of the Tenda Massif can be interpreted as related to D2 deformation during syn-collision decompression;
- The following top-to-northeast shearing (D3 and late D3) produced only partial reactivation and localized overprinting of previous fabrics.  $^{40}\text{Ar}/^{39}\text{Ar}$  ages in the range of 28–21 Ma could correspond to partial or complete reopening of phengite chronometers, during crustal-scale extension setting connected with the initiation of the rifting and drifting stages of the Ligure-Provençal basin.

Remarkably, there is no significant difference in geochronological ages across the eastern border of the Tenda Massif, between footwall and hanging wall of the supposed detachment fault, for both high ( $^{40}\text{Ar}/^{39}\text{Ar}$  on white micas) and low (apatite fission track) temperature systems (Cavazza et al., 2001; Zarki-Janki et al., 2004; Fellin et al., 2005). This agrees with the structural data presented here, which indicate a weak (low displacement) extensional-related reactivation of previous oldest and deepest fabric. In addition, the presence of clasts of Tenda-derived granitic mylonites within the lowermost part of the S.Florent sequence (see also Dallan and Puccinelli, 1995; Ferrandini et al., 1998) argues against the interpretation of the Miocene of S.Florent as a supra-detachment extensional basin related to the activity of the East Tenda shear zone at depth, as proposed by Jolivet et al. (1990) and Gueydan et al. (2003).

## 5. Discussion and conclusions

The metamorphic and structural data presented in this paper allow us to re-consider the tectonic significance of the Tertiary deformation across the eastern boundary of the Tenda Massif which, according to our new field and metamorphic data, cannot be interpreted as a core complex of Cordilleran type (Jolivet et al., 1990; Daniel et al., 1996; Gueydan et al., 2003). On the contrary, the Eastern Tenda Fault Zone shows significant structural and petrological imprints of deep seated tectonic processes associated with subduction and syn-collision intrawedge-deformation during the underthrusting of more external units. Analyses of foliation domains, heterogeneous deformation and sense of shear in mylonitized granitoids and cover rocks, coupled with petrological features of syn-kinematically developed assemblages, show that the Tenda Massif is a piece of upper continental

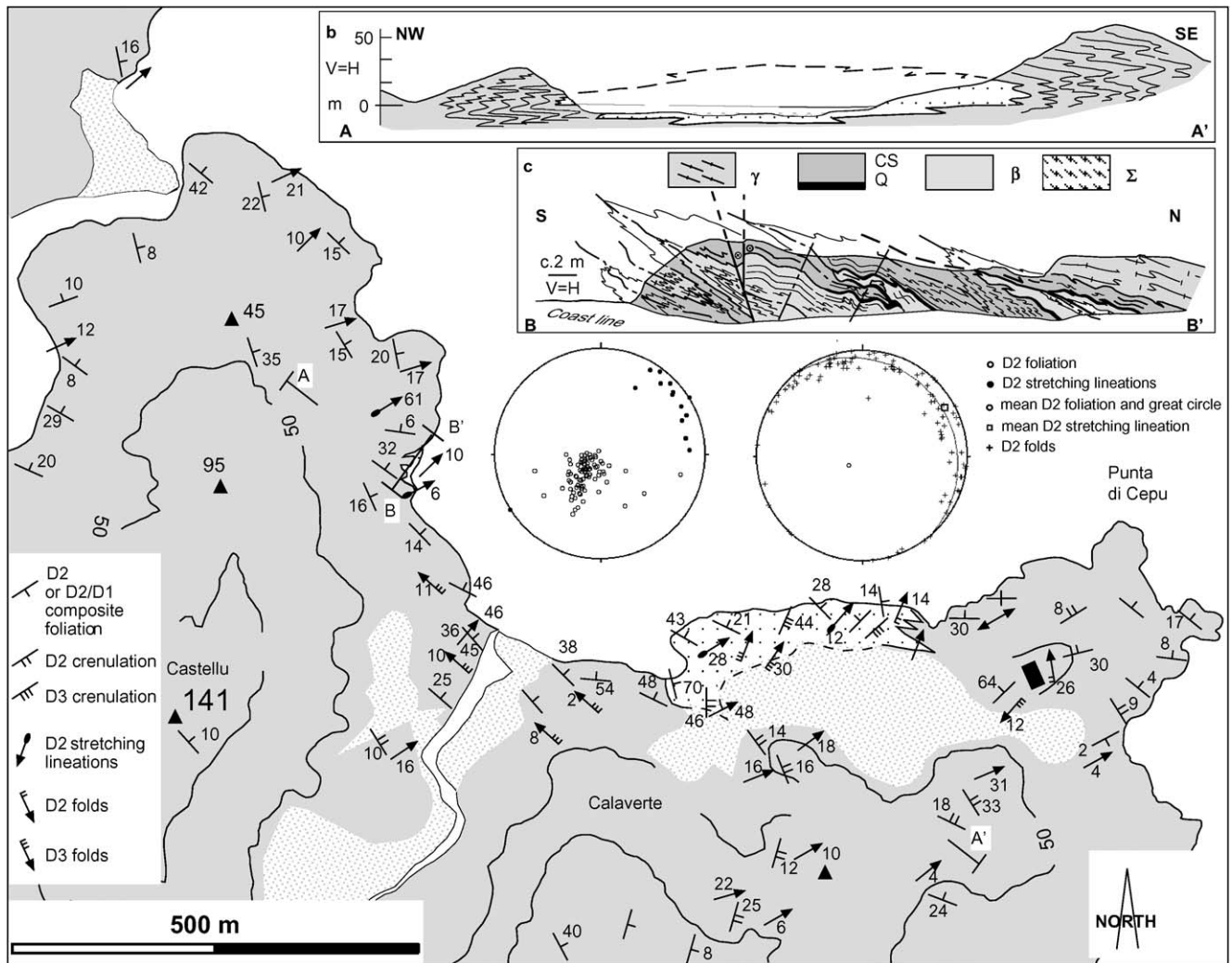


Fig. 13. Geological map of the Calaverte bay and surroundings, with inset of equal area projection plots (lower hemisphere) of pole of foliation, stretching/mineral lineation, and fold axes of D2 structures; (b) geological cross section of the Calaverte area, traced normal to the trend of D2 stretching lineation, with the interpretation of the ophiolite unit exposure within the Tenda orthogneiss as lateral termination of D2 sheath-fold; (c) schematic cross-section of north-west exposure of ophiolitic unit along the coast with observable structures (see Figs. 14c,d and 9d for micro- and meso-scale details).  $\gamma$  are orthogneiss; CS and Q are calcschists and quartzites;  $\beta$ , metabasic rocks and  $\Sigma$  actinolite-tremolite schists.

crust involved in a subduction zone (peak metamorphism at about 1.0 GPa and 450 °C), where the coupling with the ocean-derived ophiolitic unit occurred. These units shared a common retrograde structural and metamorphic history during exhumation recorded by D2 ductile fabrics in the Tenda Massif and by the large scale D2 folds in the ophiolitic units. These large scale D2 folds, involving the coupled continental and oceanic-derived units, can be framed within an orogenic wedge/subduction channel and possibly related to a process of delocalization of the strain during exhumation.

Structures similar to the large scale D2 folds described here, seem to be common in exhumed subducted continental crust. Hinterland-directed large scale folding and shearing associated with retrograde fabrics characterize the contact between basement and covers units (in some cases continental and oceanic in origin) in the Alps (e.g. Gosso et al., 1979;

Pennacchioni, 1988; Schmid et al., 1990; Wheeler and Butler, 1993; Ganne et al., 2005, 2006; Pleuger et al., 2005) and Oman (Mattauer and Ritz, 1996; Searle et al., 2004). This kind of structures, predicted in analogue and numerical modelling (Merle and Guillier, 1989; Chemenda et al., 1995; Escher and Beaumont, 1997; Allemand and Lardeaux, 1997; Malavieille et al., 1998; Kostantinovskaia and Malavieille, 2005), does not represent bulk crustal scale extension but instead reflect the relative hanging wall/footwall displacement between tectonic units within an orogenic wedge during syn-contractual exhumation of continental crust units. As in the eastern border of Tenda Massif such structures can thus be related to a complex flow pattern of rheologically heterogeneous multilayers (Schmid et al., 1990; Hippert and Tohver, 1999) during viscous extrusion, rather than post-orogenic large-scale continental crust thinning.

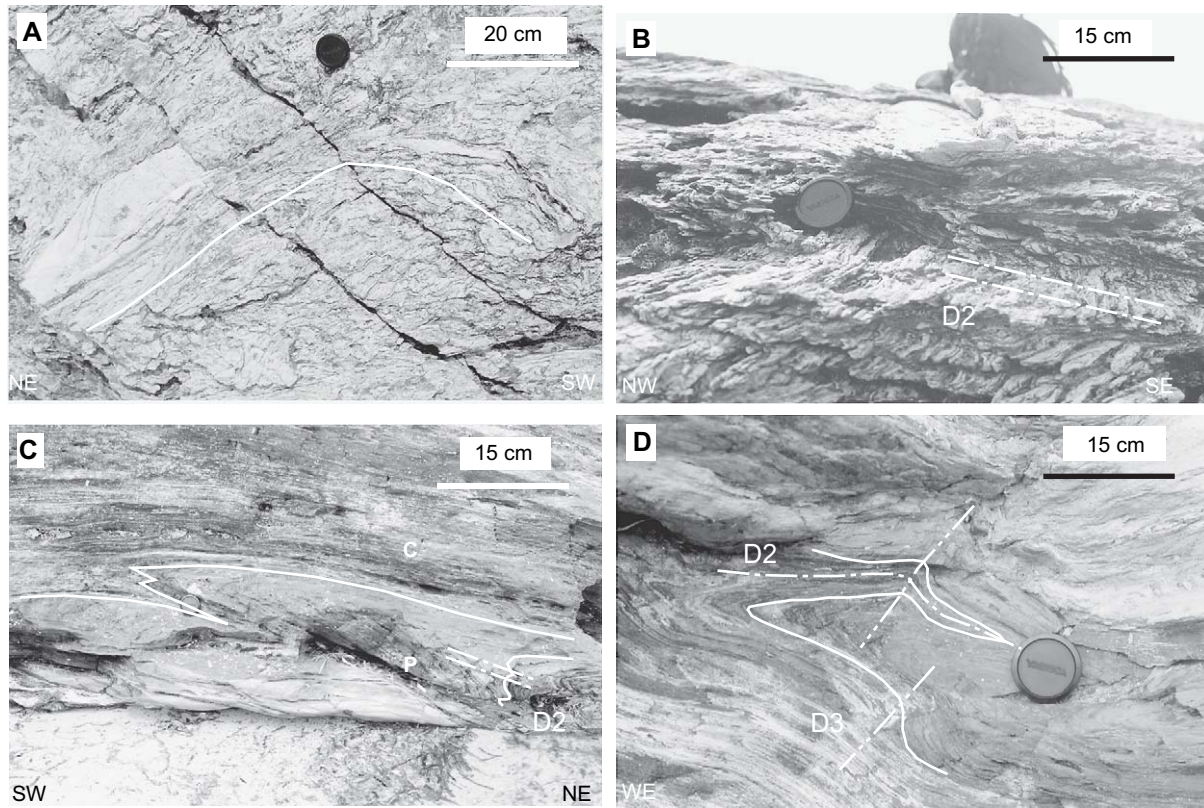


Fig. 14. (a) Orthogneiss surroundings of Punta di Cepu; curved intersection lineations and fold axes related with non-cylindrical D2 folds observed on XY plane (D2 foliation); (b) lateral (view XZ plane) of fold in (a) showing D2 fold profile and related D2 crenulation in orthogneiss; (c) D2 folds and D2 axial plane foliation of ophiolitic unit within Tenda orthogneiss (see cross section in Fig. 13c), from the bottom P are metabasic rocks and C, calcschists; and (d) interference fold structures within the ophiolitic units showing mesoscopic overprint relationships to be compared with microscale appearance in Fig. 9d.

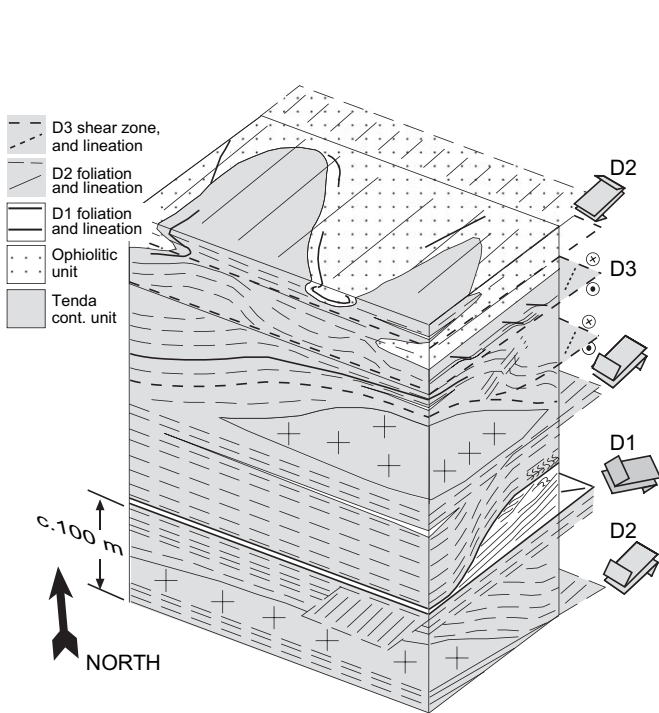


Fig. 15. Schematic interpretative structural log across the eastern border of Tenda Massif, showing relict domain of D1 shear zones and D1 foliation and the different overprinting D2 and D3 structures. The D1 contact between ophiolitic and continental Tenda unit is involved in large scale D2 sheath folds.

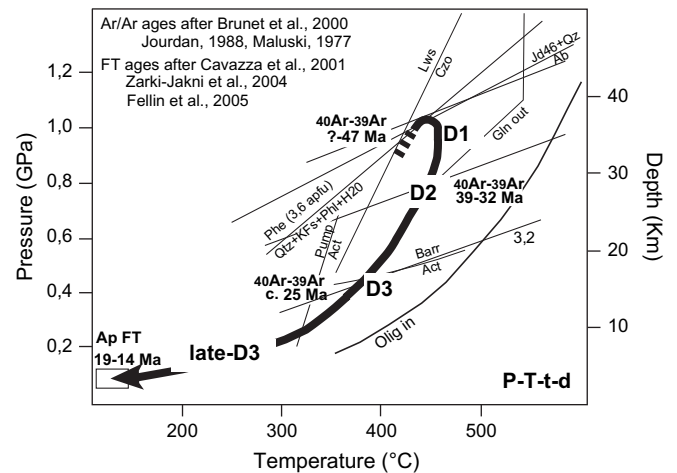


Fig. 16. Pressure-Temperature-deformation path of continental Tenda and ophiolitic units juxtaposed across the eastern border of Tenda Massif. Gln-out taken from Maresch (1977), the reaction pumpellyite + chlorite → actinolite + epidote after Liou et al. (1983), lawsonite-clinozoisite transition after Barnicoat and Fry (1986), the lower stability limit of barroisite from Ernst (1979), oligoclase-in reaction from Maruyama et al. (1983), the reaction curve for Na-clinopyroxene (Jd46) + quartz → albite was calculated with the 3.1 version of THERMOCALC program (Holland and Powell, 1998, and references therein). The reaction curve for Mg-phengite (Si = 3.6 apfu) → quartz + K-feldspar + phlogopite + H<sub>2</sub>O is after Massonne and Szpurska (1997). Ar/Ar data after Brunet et al. (2000), Jourdan (1988) and Maluski (1977). Fission track apatite ages (Ap FT) after Cavazza et al., 2001; Zarki-Janki et al. (2004) and Fellin et al. (2005).

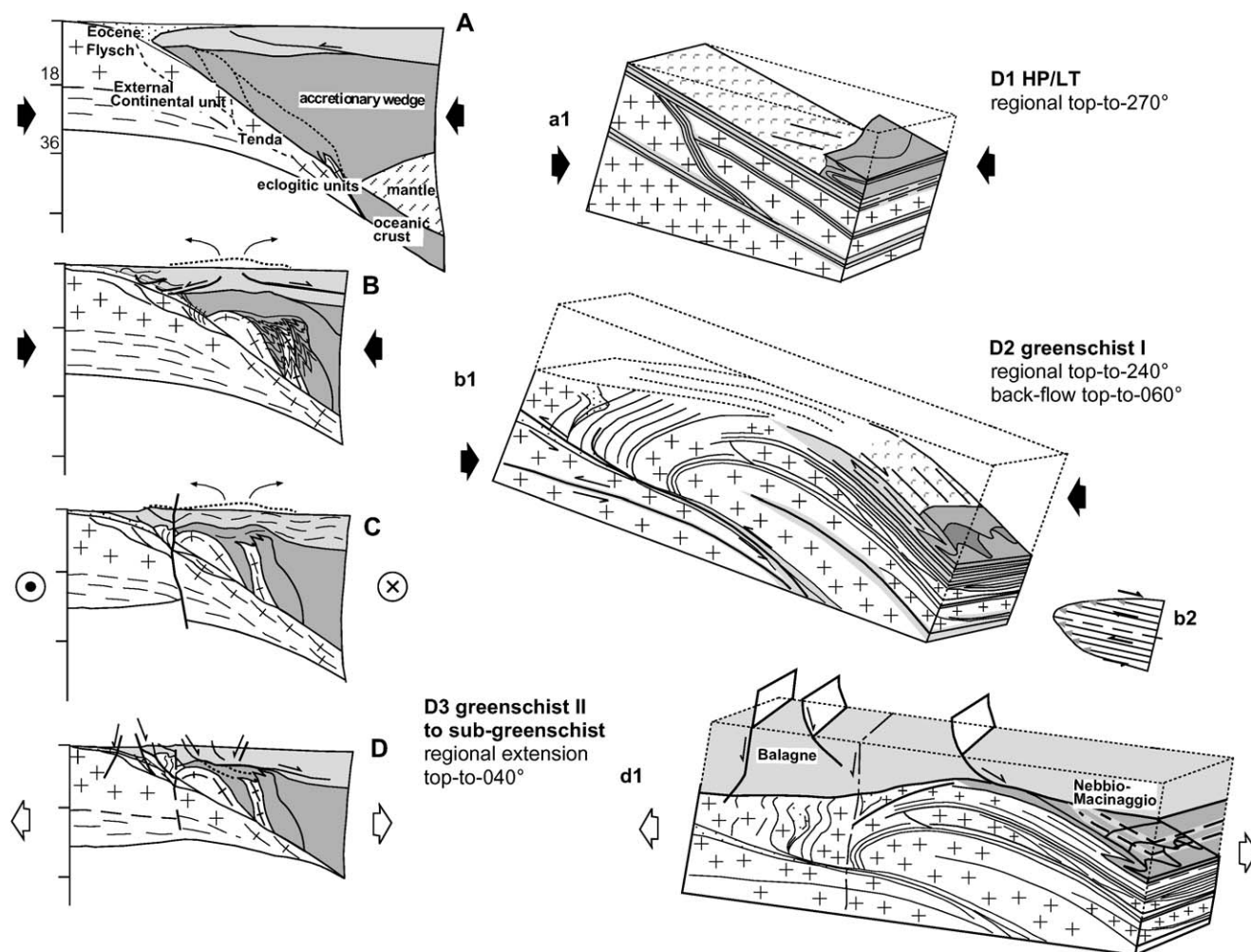


Fig. 17. Evolutionary schemes of Alpine Corsica with simplified cartoon diagrams showing the main stages of structural history of the Tenda Massif and overlying units: a) subduction of Corsican continental crust in high-pressure/low-temperature gradient with development of D1 structures in continental and ophiolitic units (a1); b) continuous shortening, underthrusting of more external continental units and syn-contraction exhumation of internal part of orogenic wedge. A crustal scale antiformal stack involving the Tenda unit developed during this stage, while erosion and low-angle normal faulting occurred in the upper part of the wedge (low-grade Balagne-Nebbio-Macinaggio nappe system). This event, post Mid Eocene in age, produced D2 fabrics (b1) in the eastern border of Tenda Massif and in the overlying ophiolitic unit. Hinterland-directed D2 shearing reflect differential displacement between continental and ophiolitic unit during viscous extrusion. b2) velocity profile (which may merely represent the deviatoric components of shear strain) resulting in a line of no shear strain (dashed) bounded by a lower top-to-west and an upper top-to-east shearing (on the basis of Merle and Guillier, 1989 and Schmid et al., 1990); c) transpressional stage (Late Eocene-early Oligocene?) with tightening of previous developed antiformal stack and further erosion-controlled exhumation; d) Late Oligocene crustal scale (trans)-extensional stage with local reactivation of previous fabrics and development of D3 and late-D3 deformations in the eastern border of the Tenda Massif (d1).

## Acknowledgements

Niko Froitzheim and an anonymous reviewer are thanked for the very useful comments and suggestions which improved the original submitted manuscript. This work was supported by MIUR (2003, 2005), University of Pisa, Pavia and CNR funds.

## References

- Allemand, P., Lardeaux, J.-M., 1997. Strain partitioning and metamorphism in a deformable orogenic wedge: application to Alpine belt. *Tectonophysics* 280, 157–169.
- Barnicoat, A.C., Fry, N., 1986. High-pressure metamorphism of the Zermatt-Saas ophiolite zone. *Journal of the Geological Society, London* 143, 607–618.
- Baudin, T., Marquer, D., Persoz, F., 1993. Basement-cover relationships in the Tambo nappe (Central Alps-Switzerland): geometry, structure and kinematics. *Journal of Structural Geology* 15 (3/5), 543–553.
- Bezert, P., 1990. Les unités alpines de la marge du Massif Cristallin Corse: Nouvelles données structurales, métamorphiques et contraintes cinématiques. Thèse de 3<sup>ème</sup> cycle, Univ. Montpellier II, France. p.385.
- Bezert, P., Caby, R., 1988. Sur l'âge post-bartonien des événements tectono-métamorphiques alpins en bordure orientale de la Corse cristalline. *Bulletin de la Société Géologique de France* 8, 965–971.
- Brunet, C., Monié, P., Jolivet, L., Cadet, J.P., 2000. Migration of compression and extension in the Thyrhenian Sea, insights from  $^{40}\text{Ar}/^{39}\text{Ar}$  ages on micas along a transect from Corsica to Tuscany. *Tectonophysics* 321, 127–155.
- Burg, J.P., Brunel, D., Gapais, G., Chen, M., Liu, G.H., 1984. Deformation of leucogranites of the crystalline Main Central Sheet in southern Tibet (China). *Journal of Structural Geology* 6, 535–542.



- Caron, J.M., 1994. Metamorphism and deformation in Alpine Corsica. *Schweizerische Mineralogische und Petrographische Mitteilungen* 7, 105–114.
- Caron, J.M., Delcey, R., 1979. Lithostratigraphie des schistes lustrés corses: diversité des séries post-ophiolitiques. *Compte Rendu Académies des Sciences*, Paris 208, 1525–1528.
- Cavazza, W., Zattin, M., Ventura, B., Zuffa, G.G., 2001. Apatite fission-track analysis of Neogene exhumation in northern Corsica (France). *Terra Nova* 13, 51–57.
- Chemenda, A., Mattauer, M., Malavieille, J., Bokun, A.N., 1995. A mechanism for syn-collisional rock exhumation and associated normal faulting: result from physical modelling. *Earth and Planetary Science Letters* 132, 225–232.
- Cohen, C.R., Schweickert, R.A., Odom, A.L., 1981. Age of emplacement of the Schistes Lustrés nappe, alpine corsica. *Tectonophysics* 72, 276–284.
- Crittenden, F.A., Coney, P.J., Davis, G.H., 1980. Cordilleran Metamorphic core complexes. *Geological Society of American Memoir* 153, 490 pp.
- Dal Piaz, G.V., Zirpoli, G., 1979. Occurrence of eclogites relics in the ophiolite nappe from Marine d'Albo, Northern Corsica. *Neues Jahrbuch für Mineralogie* 3, 118–122.
- Dallan, L., Puccinelli, A., 1995. Geologia della regione tra Bastia e St-Florent (Corsica Settentrionale). *Bollettino della Società Geologica Italiana* 114, 23–66.
- Daniel, J.M., Jolivet, L., Goffé, B., Poinsett, C., 1996. Crustal-scale strain partitioning: footwall deformation below the Alpine Oligo-Miocene detachment of Corsica. *Journal of Structural Geology* 18, 1841–1859.
- Dieni, I., Massari, F., 1982. Présence de glaucophane détritique dans le Maastriichtien inférieur de Sardaigne orientale. Implications géodynamiques. *Compte Rendu Académies des Sciences*, Paris 295, 679–682.
- Doglionni, C., Mongelli, F., Piali, G., 1998. Boudinage of the Alpine belt in the Apenninic back-arc. *Bollettino della Società Geologica Italiana* 118, 75–89.
- Durand-Delga, M., 1984. Principaux traits de la Corse Alpine et corrélations avec les Alpes Ligures. *Memorie della Società Geologica Italiana* 28, 285–329.
- Egal, E., 1992. Structures and tectonic evolution of the external zone of Alpine Corsica. *Journal of Structural Geology* 14, 1215–1228.
- Egger, C., Pinaud, M., 1998. Etude tectono-métamorphique et comparaison des styles de déformation dans le socle granitique et sa couverture des schistes lustrés en Corse septentrionale. Thèse diplôme, Université Neuchâtel, Switzerland. 211.
- Ernst, W.G., 1979. Coexisting sodic and calcic amphiboles from high-pressure metamorphic belts and the stability of barroisitic amphibole. *Mineralogical Magazine* 43, 269–278.
- Escher, A., Beaumont, C., 1997. Formation, burial and exhumation of basement nappes at crustal scale: a geometric model based on the Swiss-Italian Alps. *Journal of Structural Geology* 19, 955–974.
- Evans, M., 1990. Phase relationships of epidote-blueschists. *Lithos* 25, 3–23.
- Faccenna, C., Mattei, M., Funicello, R., Jolivet, L., 1997. Styles of back-arc extension in the Central Mediterranean. *Terra Nova* 9, 126–130.
- Faure, M., Malavieille, J., 1980. Les plis en foreau du substratum de la Nappe des Schistes Lustrés de Corse. Signification cinématique. *Compte Rendu Académies des Sciences*, Paris, Série D, 290, 1349–1352.
- Fellin, M.G., Picotti, V., Zattin, M., 2005. Neogene to Quaternary rifting and inversion in Corsica: Retreat and collision in western Mediterranean. *Tectonics* 24, TC1011, doi:10.1029/2003TC001613.
- Ferrandini, M., Ferrandini, J., Loye-Pylot, M.D., ButterlinCravette, J., Janin, M.C., 1998. Le Miocene du Bassin de Saint-Florent (Corse): Modalités de la transgression du Burdigalien Supérieur et mise en évidence du Serravalien. *Geobios* 31, 125–137.
- Fournier, M., Jolivet, L., Goffé, B., Dubois, R., 1991. The Alpine Corsica metamorphic core complex. *Tectonics* 10, 1173–1186.
- Ganne, F., Bertrand, J.-M., Fudral, S., 2005. Fold interference pattern at the top of basement domes and apparent vertical extrusion of HP rocks (Ambin and South Vanoise massifs, Western Alps). *Journal of Structural Geology* 27, 553–570.
- Ganne, F., Marquer, D., Rosenbaum, G., Bertrand, J.M., Fudral, S., 2006. Partitioning of deformation within a subduction channel during exhumation of HP-LT rocks: a case study in the Western Alps. *Journal of Structural Geology* 28, 1193–1207.
- Gibbons, W., Horak, J., 1984. Alpine metamorphism of Hercynian hornblende granodiorite beneath the blueschist facies schistes lustrés nappe of NE Corsica. *Journal of Metamorphic Geology* 2, 95–113.
- Gosso, G., Dal Piaz, G.V., Piovano, V., Polino, R., 1979. High Pressure emplacement of early-alpine nappes, post nappe deformations and structural levels. *Memorie di Scienze Geologiche* 32, 5–15.
- Gueguen, E., Doglionni, C., Fernandez, M., 1997. Lithospheric boudinage in the western Mediterranean back-arc basin. *Terra Nova* 9, 184–187.
- Gueydan, F., Leroy, Y.M., Jolivet, L., Agard, P., 2003. Analyses of continental midcrustal strain localization induced by microfracturing and reaction-softening. *Journal of Geophysical Research* 108 (B2), doi:10.1029/2001JB00611, 2003.
- Handy, M.R., Oberhänsli, R., 2004. Explanatory notes to the Map: metamorphic structure of the Alps age map of metamorphic structure of the Alps-Tectonic interpretation and outstanding problems. *Mitteilungen der Österreichischen Mineralogischen Gesellschaft* 149, 201–225.
- Harris, J., Koyi, H., Fossen, H., 2002. Mechanisms for folding of high-grade rocks in extensional settings. *Earth-Sciences Reviews* 59 (1–2), 163–210.
- Hippert, J., Tohver, E., 1999. On the development of zones of reverse shearing in mylonitic rocks. *Journal of Structural Geology* 21, 1603–1614.
- Hirth, G., Tullis, J., 1992. Dislocation creep regimes in quartz aggregates. *Journal of Structural Geology* 14, 145–159.
- Holdsworth, R.E., Butler, C.A., Roberts, A.M., 1997. The recognition of reactivation during continental deformation. *Journal Geological Society of London* 154, 73–78.
- Holland, T.J.B., Powell, R., 1998. An internally consistent thermodynamic data set for phases of petrological interest. *Journal of Metamorphic Geology* 16, 309–344.
- Jiang, D., White, J.C., 1995. Kinematics of rock flow and the interpretation of geological structures, with particular reference to shear zones. *Journal of Structural Geology* 17, 1249–1265.
- Jiang, D., Williams, P.F., 1999. A fundamental problem with the interpretation of geological structures. *Journal of Structural Geology* 21, 933–937.
- Jolivet, L., Dubois, R., Fournier, M., Michard, A., Jourdan, C., 1990. Ductile extension in Alpine Corsica. *Geology* 18, 1007–1010.
- Jolivet, L., Faccenna, C., Goffé, B., Mattei, M., Rossetti, F., Brunet, C., Storti, F., Funicello, R., Cadet, J.P., d'Agostino, N., Parra, T., 1998. Midcrustal shear zones in postorogenic extension: Example from the northern Tyrrhenian Sea. *Journal of Geophysical Research* 103 (B6), 12123–12160.
- Jourdan, C., 1988. Balagne orientale et massif du Tenda (Corse septentrionale): étude structurale, interprétation des accidents et des déformations, reconstitutions géodynamiques. Thèse de 3<sup>ème</sup> cycle, Univ. Paris-Sud, France, 246 pp.
- Kostantinovskaia, E., Malavieille, J., 2005. Erosion and exhumation in accretionary orogens: experimental and geological approaches. *Geochemistry, Geophysics, Geosystems* 6, doi:10.1029/2004GC000794, 25 pp.
- Lagabrielle, Y., 1987. Les ophiolites: marqueurs de l'histoire tectonique des domaines océaniques. Thèse de Doctorat d'Etat, Univ. Bretagne Occid., France, 316 pp.
- Lahondère, D., 1991. Les schistes bleus et les eclogites à lawsonite des unités continentales et océaniques de la Corse alpine: Nouvelles données pétrologiques et structurales. (Corse). Thèse de 3<sup>ème</sup> cycle, Univ. Montpellier II, France, 262 pp.
- Lahondère, D., Rossi, Ph., Lahondère, J.C., 1999. Structuration alpine d'une marge continentale externe: le massif du Tenda (Haute-Corse). Implications géodynamiques au niveau de la transversale Corse-Apennines. *Géologie de la France* 4, 27–44.
- Liou, J.G., Kim, H.S., Maruyama, S., 1983. Prehnite-epidote equilibria and their petrologic applications. *Journal of Petrology* 24, 321–342.
- Lister, G., Davis, G.A., 1989. The origin of metamorphic core complexes and detachment faults formed during Tertiary extension in the Colorado River Region, U.S.A. *Journal of Structural Geology* 11, 65–93.

- Malasoma, A., Marroni, M., Pandolfi, L., 2006. Evidences of subduction and exhumation of the External Continental units of “Alpine Corsica” Northern Corsica. *France* 15, 115–1130. EUG06-A-04116; TS7.4–1MO3P-0609.
- Malavieille, J., 1987. Late orogenic extension in mountain belts: insights from the Basin and Range and the Late Paleozoic Variscan belt. *Tectonics* 15 (5), 115–1130.
- Malavieille, J., Chemenda, A., Larroque, C., 1998. Evolutionary model for Alpine Corsica: mechanism for ophiolite emplacement and exhumation of high-pressure rocks. *Terra Nova* 10, 317–322.
- Maluski, H., 1977. Application des methodes de datation  $^{39}\text{Ar}/^{40}\text{Ar}$  aux minéraux des roches cristallines perturbés par les événements thermiques et tectoniques en Corse. Thèse de 3<sup>ème</sup> cycle, Univ. Montpellier, France, 300 pp.
- Maluski, H., Mattauer, M., Matte, Ph., 1973. Sur la présence de décrochement alpins en Corse. *Compte Rendu Académies des Sciences, Paris, série D* 276, 709–712.
- Mancktelow, N., 1985. The Simplon line: a major displacement zone in the western Lepontine Alps. *Eclogae geologicae Helvetiae* 78, 73–96.
- Maresch, W.V., 1977. Experimental studies on glaucophane: an analysis of present knowledge. *Tectonophysics* 43, 109–125.
- Marquer, D., Challandes, N., Baudin, T., 1996. Shear zone patterns and strain distribution at the scale of a Penninic Nappe; the Suretta Nappe (eastern Swiss Alps). *Journal of Structural Geology* 18, 753–764.
- Marroni, M., Pandolfi, L., 2003. Deformation history of the ophiolite sequence from the Balagne Nappe, northern Corsica: insights in the tectonic evolution of Alpine Corsica. *Geological Journal* 38, 67–83.
- Maruyama, S., Suzuki, K., Liou, J.G., 1983. Greenschist-amphibolite transition equilibria at low pressures. *Journal of Petrology* 24, 583–604.
- Massonne, H.J., Schreyer, W., 1987. Phengite geobarometry based on the limiting assemblage with K-feldspar, phlogopite, and quartz. *Contributions to Mineralogy and Petrology* 96, 212–224.
- Massonne, H.J., Szpurska, Z., 1997. Thermodynamic properties of white micas on the basis of high-pressure experiments in the systems K2O-MgO-Al2O3-SiO2-H2O and K2O-FeO-Al2O3-SiO2-H2O. *Lithos* 41, 229–250.
- Mattauer, M., Ritz, J.-F., 1996. Arguments géologiques en faveur d’un modèle de subduction continentale pour l’exhumation du métamorphisme haute-pression d’Oman. *Compte Rendu Académies des Sciences, Paris, série IIA* 322, 869–876.
- Mattauer, M., Faure, M., Malavieille, J., 1981. Transverse lineation and large-scale structures related to Alpine obduction in Corsica. *Journal of Structural Geology* 3, 401–409.
- Merle, O., Guillier, B., 1989. The building of Swiss central Alps: an experimental approach. *Tectonophysics* 165, 41–56.
- Molli, G., Tribuzio, R., 2004. Shear zones and metamorphic signature of subducted continental crust as tracers of the evolution of the Corsica/Northern Apennine orogenic system. In: Alsop, I., Holdsworth, R.E., McCaffrey, J.W., Hand, M. (Eds.), *Flow Process in Faults and Shear Zones*. Geological Society of London, Special Publication 224, 321–335.
- Molli, G., Malasoma, A., Meneghini, F., 2005. Brittle precursors of HP/LT microscale shear zone: a case study from Alpine Corsica, 15<sup>th</sup> Conference on Deformation mechanisms, Rheology and Tectonics, ETH Zurich, 2–4 May 2005, Abstract volume 153.
- Nussbaum, C., Marquer, D., Biino, G.G., 1998. Two subduction events in a polycyclic basement: Alpine and pre-Alpine high-pressure metamorphism in the Suretta nappe, Swiss eastern Alps. *Journal of Metamorphic Geology* 16/5, 591–605.
- Ohnenstetter, M., Rossi, Ph., 1985. Reconstitution d’une paléochambre magmatique exceptionnelle dans le complexe basique-ultrabasique du Tenda, Corse hercynienne. *Compte Rendu Académies des Sciences, Paris, série II* 300, 853–858.
- Passchier, C., 1984. The generation of ductile and brittle shear bands in a low-angle mylonite zone. *Journal of Structural Geology* 6, 273–281.
- Passchier, C., 1997. The Fabric attractor. *Journal of Structural Geology* 19, 113–127.
- Pennacchioni, G., 1988. Studio geologico del tratto meridionale della dorsale tra Valnontey e Valleile (Cogne, Valle d’Aosta). *Memorie Scienze Geologiche* 40, 333–354.
- Pequignot, G., Lardeaux, J.M., Caron, J.M., 1984. Recristallisation d’éclogites de basse température dans les metabasites corses. *Compte Rendu Académies des Sciences, Paris, série II* 299, 871–874.
- Platt, J.P., 1986. Dynamics of orogenic wedges and the uplift of high-pressure metamorphic rocks. *Geological Society of American Bulletin* 97, 1037–1053.
- Pleuger, J., Froitzheim, N., Jansen, E., 2005. Folded continental and oceanic nappes on the southern side of Monte Rosa (Western Alps, Italy): anatomy of a double collision suture. *Tectonics* 24, TC4013, 22 pp.
- Ring, U., Brandon, M.T., Willet, S.D., Lister, G.S., 1999. Exhumation processes. In: Ring, U., Brandon, M.T., Lister, G.S., Willet, S.D. (Eds.), *Exhumation Processes: Normal Faulting, Ductile Flow and Erosion*. Geological Society, London, Special Publication 154, 1–27.
- Rollet, N., Deverchère, J., Beslier, M.-O., Guennoc, P., Réhault, J.-P., Sossou, M., Truffet, C., 2002. Back arc extension, tectonic inheritance, and volcanism in the Ligurian Sea, Western Mediterranean. *Tectonics* 21, 1–23.
- Rosenbaum, G., Regenauer-Lieb, K., Weinberg, R., 2005. Continental extension: from core complexes to rigid block faulting. *Geology* 33 (7), 609–612.
- Rossetti, F., Faccenna, C., Jolivet, L., Goffé, B., Funicello, R., 2002. Structural signature and exhumation P-T-t paths of the blueschist units exposed in the interior of the Northern Apennine chain, tectonic implication. *Bollettino della Società Geologica Italiana, volume speciale n.1* 20, 829–842.
- Rossi, Ph., Cocherie, A., Lahondère, D., 1992. Relations entre les complexes mafiques-ultramafiques et le volcanisme andésitique stéfano-permien de Corse occidentale, témoins des phénomènes d’amincissement crustal néo-varisques. *Compte Rendu Académies des Sciences, Paris, série II* 315, 1341–1348.
- Rossi, Ph., Lahondère, J.C., Luch, D., Loye-Pilot, M.D., Jacquet, M., 1994. Carte géologique de la France à 1/50.000, feuille Saint-Florent. BRGM.
- Rossi, Ph., Durand Delga M., Lahondère, J.C., Lahondère, D., 2003. Carte géologique de la France à 1/50.000, feuille Santo Pietro di Tenda. BRGM.
- Schmid, S.M., Haas, R., 1989. Transition from near-surface thrusting to intrabasin decollement, Schling Thrust, Eastern Alps. *Tectonics* 8, 697–718.
- Schmid, S.M., Aeble, H.R., Heller, F., Zingg, A., 1989. The role of Periadriatic Line in the Tectonic evolution of the Alps. In: Coward, M.P., Dietrich, D., Park, P.G. (Eds.), *Alpine Tectonics*. Geological Society, London, Special Publication 45, 153–171.
- Schmid, S.M., Ruck, Ph., Schreurs, G., 1990. The significance of the Schams nappe for the reconstruction of the paleotectonic and orogenic evolution of the Pennine zone along the NFP-20 East traverse (Grisons, eastern Switzerland). In: Roure, F., Heitzmann, P., Polino, R. (Eds.), *Deep Structure of the Alps*. *Mém. Soc. géol. Fr.*, Paris, 156; *Mém. Soc. géol. Suisse, Zurich*, 156; Vol. Spec. Soc. Geol. It, 1, pp. 263–287.
- Searle, M.P., Warren, C.J., Waters, D.J., Parrish, R.R., 2004. Structural evolution, metamorphism and restoration of the Arabian continental margin, Saih Hatat region, Oman Mountains. *Journal of Structural Geology* 26, 451–473.
- Selverstone, J., 1985. Petrologic constraints on imbrication, metamorphism and uplift in the SW Tauren window, Eastern Alps. *Tectonics* 4, 687–704.
- Spear, F.S., 1993. *Metamorphic Phase Equilibria and Pressure-Temperature-Time Paths*. Mineralogical Society of America, Washington, D.C., 799 pp.
- Speranza, F., Villa, I.M., Sagnotti, L., Florindo, F., Cosentino, D., Cipollari, P., Mattei, M., 2002. Age of the Corsica-Sardinia rotation and Ligure-Provençal Basin spreading: new paleomagnetic and Ar/Ar evidence. *Tectonophysics* 657/1, 112–133.
- Tribuzio, R., Giacomini, F., 2002. Blueschist facies metamorphism of peralkaline rhyolites from the Tenda crystalline massif (northern Corsica): evidence for involvement in the Alpine subduction event? *Journal of Metamorphic Geology* 20, 513–526.
- Warburton, J., 1986. The ophiolite-bearing Schistes lustrés nappe in Alpine Corsica: a model for emplacement of ophiolites that have suffered

- HP/LT metamorphism. *Geological Society of America Memoir* 164, 313–331.
- Waters, C.N., 1990. The Cenozoic tectonic evolution of alpine Corsica. *Journal of the Geological Society, London* 147, 811–824.
- Wernicke, B., 1981. Low-angle normal faults in the Basin and Range Province: nappe tectonics in extending orogen. *Nature* 291, 645–648.
- Wheeler, J., Butler, R.W.H., 1993. Evidence for extension in the western Alpine orogen: the contact between the oceanic Piemonte and overlying continental Sesia units. *Earth and Planetary Science Letters* 117, 457–474.
- Wheeler, J., Butler, R.W.H., 1994. Criteria for identifying structures related to true crustal extension in orogens. *Journal of Structural Geology* 16, 1023–1027.
- Zark-Janki, B., van der Beek, P., Popeau, G., Sosson, M., Rossi, P., Ferrandini, J., 2004. Cenozoic denudation of Corsica in response to Ligurian and Thyrrenian extension: results from apatite fission track thermochronology. *Tectonics* 23, TC1003, doi:10.1029/2003TC001535.